nature communications

Article

https://doi.org/10.1038/s41467-025-64854-5

Extended fear learning enhances excitatory and inhibitory synaptic transmission onto amygdala engram cells

Received: 6 December 2023

Accepted: 9 September 2025

Published online: 11 November 2025

Check for updates

Deborah Daphne[1,2], Ashutosh Ahire[1,2], Shelly P. Singh[1], Shlomo Wagner[1], Edi Barkai[1] & Iris Reuveni[1]

If a fear engram is too crucial to be ignored, its strength must be amplified to allow it to dominate behavior. Here we report a learning-induced amplification mechanism that promotes an engram to dominance. The amplification mechanism is mediated by CaMKII-dependent increase of the conductance of all AMPA and $GABA_A$ channels in each of the neurons that compose the engram in male mice. Moreover, we show that only crucial fear engrams are amplified and that the amplification mechanism is induced days after training completion. The engram amplification is correlated with intense and enduring freezing response upon retrieval; blocking the amplification dramatically reduces the freezing response. Thus, days after training, engrams that encode crucial information are promoted to dominance through the induction of the amplification mechanism. We introduce a learning functionality in which the strength of a critical engram is biasedly increased, therefore ensuring its dominance of the behavioral response.

External events and implicit mental processes are encoded by the activity of subpopulations of neurons, termed engram cells. The cells composing a learned engram are reactivated by specific cues associated with the training experience and their stimulation can directly elicit memory recall[1–7]. Accordingly, in the past decade it was established that learning is expressed in the induction of immediate early genes (IEGs) in a subset of neurons, and that this is tied to encoding[8] and subsequent retrieval of the memory engram[3,9]. For example, it was shown that the freezing response in mice trained in a fear conditioning paradigm is correlated with the activity of IEGs expressing cells in the lateral amygdala (LA)[1,10].

As well as encoding a stimulus, an engram also encodes the intensity of that stimulus. Accordingly, in the visual cortex[11], piriform cortex[12], auditory cortex[13,14] and other high brain areas[15,16], increasing the intensity of the sensory stimulus enhances the firing response of the encoding neurons, which was shown to increase the impact on the behavioral outcome[17,18]. Taken together, selectively increasing the firing response of an evoked engram establishes a learning concept in which the power of the engram is preferentially increased, thus enabling it to dominate the behavioral outcome. Enhancement of the response of an evoked engram has been theoretically suggested to result in dominant memories; once the amplified engram is activated it would "take over" the activity in the brain areas where it resides[19] and become able to dominate the behavioral outcome[20].

We have previously shown computationally that whole-cell multiplication of the strength of all inhibitory and excitatory synaptic inputs to a neuron directly results in multiplication of the number of spikes it generates, a phenomenon termed the "amplification mechanism"[19,21] (Supplementary Fig. 1). Notably, if the amplification mechanism is selectively induced in each of the cells that compose an engram, it should selectively increase the firing response of the engram, and thus can act as an engram amplification mechanism (Supplementary Fig. 1).

A mechanism for engram amplification is a concept that extends beyond the well-studied activity-dependent synaptic plasticity that has been suggested as underlying long-term memory formation in several key points: (1) the engram amplification mechanism intensifies the response of an already formed engram rather than forming new

[1]Sagol Department of Neurobiology, Faculty of Natural Sciences, University of Haifa, Haifa, Israel. [2]These authors contributed equally: Deborah Daphne, Ashutosh Ahire. e-mail: ireuve02@gmail.com

associations between the different inputs. (2) The increased synaptic excitation that underlies the engram amplification is not synapse specific, but rather cell specific. (3) Unlike Hebbian learning, the engram amplification mechanism requires a parallel and similar increase in the strength of synaptic inhibition.

Since engram amplification is independent of its formation, it has the potential to be induced on only a fraction of the engrams. This enables the amplified engram to largely exceed the power of other non-amplified engrams and thus to implement and maintain task-specific bias. This led us to expect that the amplification mechanism will only be induced on engrams that are perceived as highly critical for survival.

Here, we show that intense fear conditioning results in a long-lasting and resilient fear response. Subsequently, we show at the cellular level that such a response is mediated through the induction of an amplification mechanism on virtually all the neurons that were active during the retrieval of the fear engram: thus, the strength of all synaptic inputs (inhibitory and excitatory) onto these neurons was uniformly multiplied by a factor of nearly two. We then identify the precise biophysical and molecular mechanism that underlies the amplification mechanism. Finally, we show how the power of the amplified fear engram is dramatically reduced by using precise pharmacological tools that target the amplification mechanism. Our results pave a clear way for specifically reducing the intensity of long-lasting traumatic memories.

Results

We explored the cellular mechanisms underlying the induction of long-lasting dominant fear memories by using two fear-conditioning paradigms. The first is an extensive training paradigm, in which mice are conditioned for two consecutive days, and a milder training paradigm in which mice are conditioned for one day only. The fear engram was retrieved at different time points after the conditioning and the freezing response was compared between the two conditioning paradigms.

We found that the extensive training paradigm resulted in a much more robust and persistent fear response compared with the mild training. The mice trained with the extensive conditioning paradigms ($n = 9$ mice) exhibited an intense and long-lasting freezing response that remained high for 6 weeks, while mice trained in the mild paradigm ($n = 7$ mice) exhibited a steep drop in the freezing response just 5 days after fear conditioning (Fig. 1A). The difference in freezing time was apparent starting from the first day after training completion and became highly pronounced in the next 6 weeks. Notably, the freezing time in the extensively paired group was not reduced during the period of 5–45 days after conditioning ($F_{3,8} = 1.69$, $P = 0.19$). The freezing response exhibited a sharp reduction 60 days after conditioning, which led to a similar freezing response in the two paradigms.

Only arc+ neurons from the extensively paired group expressed a whole-cell increase in synaptic strength 5 days after fear conditioning

Next, we examined whether an amplification of the fear engram that is acquired during extensive training underlies the intense long-lasting freezing response 5 days after training, which is when the freezing response became highly differentiated between the extensively and mildly trained groups.

To visualize LA neurons recruited during retrieval of the fear engram, we utilized a mouse line expressing destabilized *Venus* fluorescent protein (*dVenus*) under the control of a transgenic *arc* promoter (*arc::dVenus* mice)[22], thereby allowing a selective tagging of recently activated engrams, and leaving the endogenous *arc* genes unmodified. The expression of *arc::dVenus* was previously shown to correlate with fear engram expression in the LA, where *arc::dVenus* was selectively expressed in principle excitatory cells and showed high colocalization with the endogenous *arc*[22].

Using histological techniques, we first showed that the fear engram was maintained in the LA 5 days after training, as evidenced by the higher numbers of neurons that were stained with *arc* in each section in the extensively paired group as compared with the unpaired group (averaged number of cells counted using histological techniques per section: unpaired, 2.3 ± 0.5 [$n = 4$ mice] vs paired 14.4 ± 7.5 [$n = 3$ mice]; $P = 0.039$).

To examine whether the amplification mechanism is induced on the *arc*+ neurons in the paired group we recorded miniature inhibitory and excitatory synaptic currents from pyramidal cells in the LA, using whole-cell patch clamp recording. Neurons were recorded from brain slices from four experimental groups: naïve, unpaired, paired after extensive training (two training days) and paired after mild training (one training day).

The miniature synaptic events are evoked by spontaneous release of vesicles in the presynaptic site and, therefore, do not reflect pathway-dependent activity. This enables us to examine the learning-induced modifications within the scope of whole-cell synaptic modulation. To allow the identification of LA neurons recruited during retrieval of the fear engram, we recorded *arc::dVenus*-expressing cells (*arc* +) and their neighboring cells that do not express *arc*::dVenus (*arc*−) (Fig. 1B). As previously reported[22], *arc*+ neurons in naïve mice were significantly more excitable than *arc*− neurons. The average spike number evoked in labeled neurons (14.4 ± 2.5, $n = 13$) was significantly higher ($P < 0.05$; $n = 5$ mice) than the average number in non-labeled neurons (8.5 ± 2.7, $n = 13$) (Fig. 1B).

arc+ neurons recorded 5 days after fear conditioning in slices taken from extensively trained mice only ($n = 8$ mice), showed significantly enhanced mean amplitude of miniature spontaneous inhibitory events (mIPSCs, Fig. 1C) compared with *arc*− neurons from the same slices (24.8 ± 2.9 [$n = 14$] in *arc*+, compared with 16.9 ± 2 pA [$n = 18$] in *arc* −, $P < 0.001$). The mean amplitude of mIPSCs in *arc*+ vs *arc*− was similar in neurons from mildly trained mice (16.1 ± 3.1 [$n = 9$] in *arc* +; 17.4 ± 2.8 pA [$n = 8$] in *arc* −, $P = 0.39$; $n = 7$ mice), naïve mice (17.2 ± 2.6 [$n = 17$] in *arc* +; 18.3 ± 1.8 pA [$n = 10$] in *arc* −, $P = 0.25$; $n = 6$ mice) and unpaired mice (17.3 ± 2.9 [$n = 10$] in *arc* +; 18.3 ± 1.8 pA [$n = 9$] in *arc* −, $P = 0.92$; $n = 6$ mice).

A similar observation was made for synaptic excitation. As shown in Fig. 1D, *arc*+ neurons recorded in slices taken from extensively trained mice only, showed significantly enhanced mean amplitude of miniature spontaneous excitatory events (mEPSCs), compared with *arc*− neurons from the same slices (13.9 ± 1.0 [$n = 14$], compared with 7.9 ± 0.8 pA [$n = 14$], $P < 0.001$; $n = 6$ mice). The mean amplitude of mEPSCs in *arc*+ vs *arc*− was similar in neurons from mildly trained mice (8.2 ± 1.6 [$n = 8$] in *arc* +; 8.1 ± 0.9 pA [$n = 7$] in *arc* −, $P = 0.82$; #mice=6), naïve mice (8.1 ± 0.9 [$n = 7$] in *arc* +; 8.0 ± 0.7 pA [$n = 1$] in *arc* −, $P = 0.8$; #mice=4) and unpaired mice (8.4 ± 0.7 [$n = 6$] in *arc* +; 7.9 ± 0.2 pA [$n = 6$] in *arc* −, $P = 0.08$; #mice=4). The frequency of events was not modified between groups (Table 1), indicating that extensive training was not followed by pre-synaptic changes 5 days after training.

Thus, extensive, but not mild, fear conditioning manifests long-lasting, profound enhancement of inhibitory and excitatory synaptic inputs selectively onto *arc*+ neurons. Neighboring *arc*− cells were not modified by extensive fear conditioning and exhibited similar values to the control groups. These findings support the notion that the amplification mechanism is induced on neurons that compose crucial engrams only, where the increased synaptic excitation is paralleled by increased synaptic inhibition. Moreover, the lack of enhancement in the *arc*+ cells of control groups shows that *arc* expression alone is not sufficient to induce the increase in synaptic strength.

https://doi.org/10.1038/s41467-025-64854-5

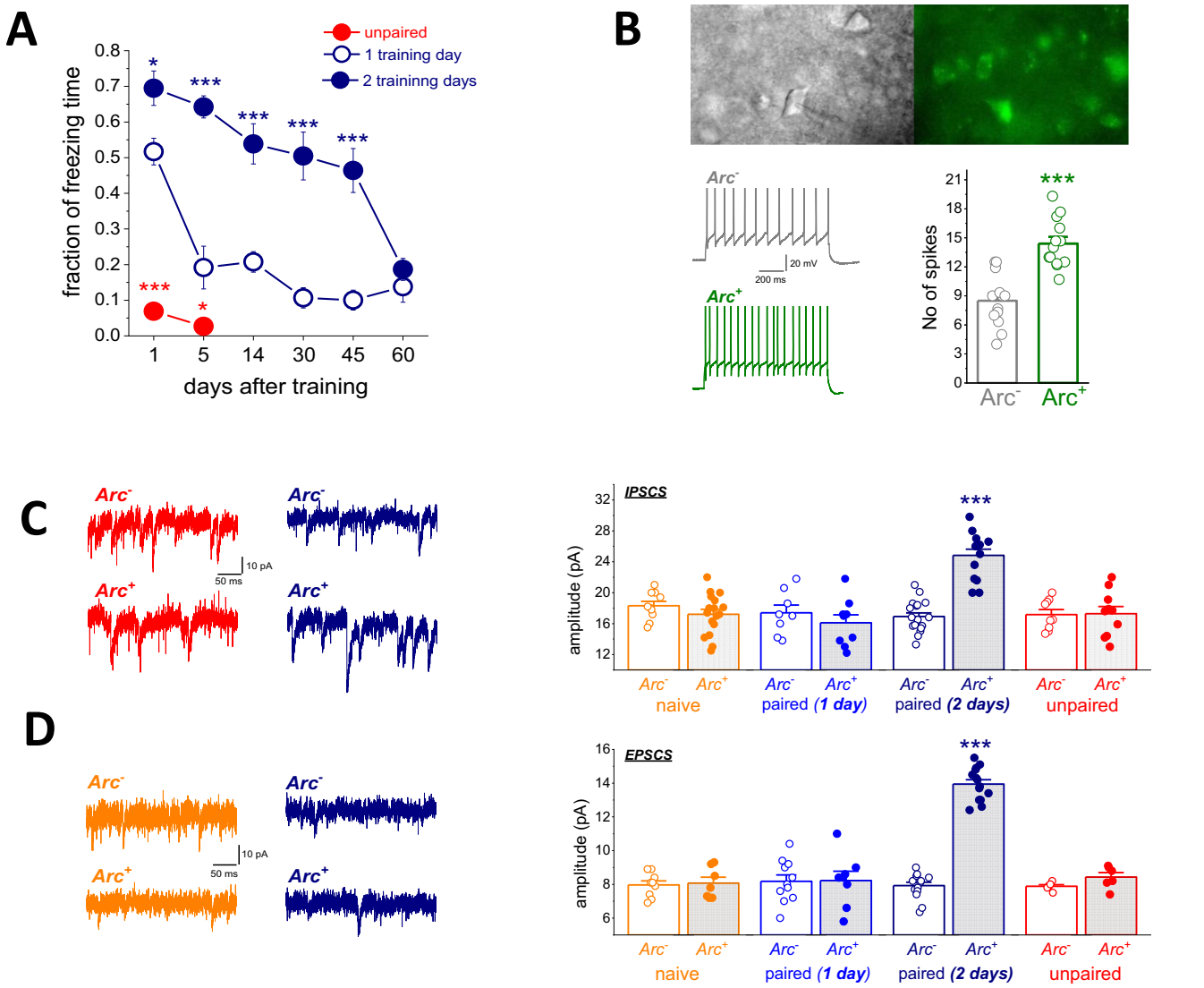

Fig. 1 | Long-lasting fear conditioning is accompanied by enhanced synaptic transmission onto arc+ labelled neurons. A The extensively trained group that was conditioned for two consecutive days exhibited persistent and strong freezing as compared with the mildly conditioned group, which was conditioned for 1 day only. The fear engram was retrieved by presentation of tone only, in a different context on 1, 5, 14, 45 and 60 days after fear training (the difference between groups was tested using two-sides t-test and has the following P values ordered by the different days ($P = 0.031$; $P = 0.0006$; $P = 0.0003$; $P = 0.0001$; $P = 0.001$; $P = 0.22$). **B** Top: slices taken from the LA of *arc::dVenus* mice 5 days after training. *arc*-expressing cells were identified based on high fluorescence. Bottom: The firing frequency was higher ($T_{1,24} = -5.24$; $P = 0.0058$) in *arc*+ than *arc*− neurons. Each point represents the number of spikes in a single cell. Left: Representative traces of miniature synaptic inhibitory (**C**) and excitatory (**D**) events from *arc*+ neurons (bottom) and *arc*− neurons (top) recorded from unpaired (red), naïve (orange) and extensively paired (blue) groups. Right: The average amplitude of the mIPSCs (**C**) and mEPSCs (**D**) from *arc*+ neurons in the extensively paired group was larger than in the *arc*− neurons and in the naïve, mildly paired, extensively paired and unpaired groups. Each point represents the averaged PSC amplitude in a single cell. Two-way ANOVA. mIPSCs: *arc*: $F_{1,78} = 4.9$; $p = 0.029$; groups (naïve, unpaired, extensively paired, mildly paired): $F_{3,78} = 11.8$; $p = 6 \times 10^{-6}$. Interaction: $F_{3,78} = 15.2$; $p = 0.0000008$. mEPSCs: *arc:* $F_{1,55} = 55.5$; $p = 6.8 \times 10^{-8}$. Groups: $F_{3,55} = 43.2$; $p = 1.7 \times 10^{-14}$. Interaction: $F_{3,55} = 42.4$; $p = 2.4 \times 10^{-14}$. Bars represent mean ± SE. (*$P < 0.05$; ***$P < 0.001$).

Enhanced synaptic strength is mediated by increased synaptic channel conductance

The amplitude of a synaptic event is determined by the number of synaptic channels and by the current that is conducted by each of these channels. Thus, uniform scaling of the strength of all synapses can be implemented either through multiplication of the number of synaptic receptors by a constant factor, or through modulation of the conductance of the synaptic channels. Using non-stationary fluctuation analysis (NSFA) we measured for each cell the mean current that is mediated by a single synaptic channel and the number of synaptic channels that mediates a mean synaptic event. We found that the mean single channel current, but not the mean number of channels that underlies synaptic events, was selectively increased in *arc*+ cells from extensively paired animals, both for inhibition (Fig. 2A–C) and excitation (Fig. 2D–F).

In *arc*+ neurons from extensively trained mice the mean inhibitory channel current was 1.9 ± 0.33 pA ($n = 14$), a significantly higher value ($P < 0.001$, $n = 7$ mice) than the mean value in *arc*− neurons (1.06 ± 0.17 pA [$n = 12$]) (Fig. 2B). No significant difference was found in neurons from naïve animals (1.11 ± 0.24 [$n = 10$] in *arc*+ neurons; 1.09 ± 0.2 pA [$n = 14$] in *arc*− neurons; $P = 0.81$; $n = 5$ mice); unpaired animals (n-5 mice; *arc* +: 1.06 ± 0.19 [$n = 9$]; *arc* −: 1.05 ± 0.17 pA [$n = 7$]) or mildly trained animals ($n = 6$ mice; *arc* +: 0.98 ± 0.16 [$n = 5$]; *arc* −: 1.1 ± 0.21 pA [$n = 5$]). The mean number of channels activated by the inhibitory events (Fig. 2B) was significantly smaller ($P < 0.05$) for *arc*+ neurons from extensively trained mice, where the mean number for *arc*+

neurons was 15.9 ± 2.8 (n = 14), compared with 18.5 ± 2.9 (n = 11) for *arc* − neurons. For naïve mice the mean number of channels for *arc*+ neurons was 18.1 ± 3.8 (n = 18) and for *arc*− neurons was 18.6 ± 4.3 (n = 8) (P = 0.77); for unpaired animals: arc +: 18 ± 2.4 (n = 9); *arc* −: 18.6 ± 3.3 (n = 7); and for mildly trained animals: *arc* +: 18 ± 4 (n = 5); *arc* −: 18.8 ± 2.8 (n = 5).

Similar learning-induced changes were observed for excitatory currents (Fig. 2E, F). In *arc*+ neurons from extensively trained mice the average excitatory channel current was 1.7 ± 0.38 pA (n = 8), a significantly higher value P < 0.001; n = 4 mice) than the mean value in *arc* − neurons (0.84 ± 0.16 pA [n = 8]). No significant difference was found in neurons from naïve animals (n = 4 mice; 0.96 ± 0.17 (n = 4) in *arc*+ neurons vs 0.92 ± 0.12 pA (n = 6) in *arc*− neurons (P = 0.66); unpaired: n = 3 mice; *arc* +: 0.92 ± 0.06 (n = 4); *arc* −: 0.93 ± 0.15 pA (n = 4); mildly trained: n = 5 mice; *arc* +: 0.98 ± 0.23 (n = 5); *arc* −: 0.88 ± 0.19 pA (n = 5). The mean number of channels that mediates the excitatory events was similar for all groups (Fig. 2E, F). For extensively trained mice the mean number of channels for *arc*+ neurons was 10.5 ± 1.7 (n = 8) and for *arc*− neurons was 11.8 ± 1.8 (n = 8), (P = 0.19). For naïve mice the mean number of channels for *arc*+ neurons was 12.3 ± 2.5 (n = 4) and for *arc*− neurons was 11.2 ± 1.8 (n = 5), (P = 0.48); for unpaired: *arc* +: 12.7 ± 0.87 (n = 4); *arc* −: 10.6 ± 2.1 (n = 4); mildly trained: *arc* +: 11.8 ± 2.3 (n = 5); *arc* −: 13.8 ± 1.3 (n = 5).

We conclude that the increased amplitude of the synaptic events was mediated by increased conductance of the synaptic channels for both inhibition and excitation.

Table 1 | comparison of the frequency of the events (raw headers) of synaptic events recorded from *arc*+ cells and from *arc- cells*

IPSCS	Events frequency #events/min	*arc* +	*arc*−	*P* value
	Extensively trained group	275 ± 85	245 ± 109	0.5
	Mildly trained group	190 ± 98	225 ± 76	0.41
	Naïve group	210 ± 77	217 ± 103	0.82
	Unpaired group	275 ± 169	288 ± 118	0.85
EPSCS	Events frequency #events/min			
	Extensively trained group	110 ± 58	113 ± 71	0.21
	Mild training group	88 ± 93	104 ± 63	0.44
	Naïve group	123 ± 113	107 ± 74	0.54
	Unpaired group	113 ± 44	103 ± 33	0.51

Enhancement of synaptic strength induced by extensive fear training appears 5 days after learning

Next, we examined the temporal properties of the profound synaptic enhancement described above in the *arc*+ labeled neurons from the extensively trained group. We found that although extensively trained mice exhibit a strong fear engram 1 day after training completion (Fig. 1A), the synaptic strength of both inhibitory and excitatory inputs does not show any enhancement until the 5 days after training (Fig. 3A_2, B_2). For inhibitory synaptic currents, the average amplitude 1 day after extensive fear conditioning was in fact significantly smaller (P = 0.0048; n = 6 mice) in *arc*+ neurons (14.0 ± 2.5 pA, n = 12) compared with *arc*− neurons (17.7 ± 2.1 pA, n = 7). Three days after conditioning, the average amplitude of mIPSCs in *arc*+ neurons and *arc*− neurons was similar (P = 0.9; n = 4 mice, 16.3 ± 3.2, [n = 8] in *arc*+ neurons vs 16.5 ± 2.5 pA [n = 6] in *arc*− neurons). For unpaired mice and mildly trained mice, the mean mIPSC amplitude remained stable and similar to the mean values in neurons from naïve mice throughout this time period (Fig. 3A_2, A_3).

Enhanced synaptic excitation was also not apparent 1 and 3 days after extensive fear conditioning (Fig. 3B_2). One day and three days after training, the average amplitude of mEPSCs in *arc*+ and *arc*− neurons was similar (1 day: P = 0.3; n = 3 mice, 7.9 ± 1.6 [n = 10] in *arc*+ neurons vs 7.5 ± 0.9 pA [n = 9] in *arc*− neurons; 3 days: P = 0.31; n = 3 mice, 8.6 ± 0.8 in *arc*+ neurons [n = 10] vs 7.9 ± 0.9 pA [n = 8] in *arc*− neurons). The mean mEPSC amplitude in neurons from unpaired mice and mildly trained mice remained stable and similar to the mean values in neurons from naïve mice throughout this time period (Fig. 3B_2, B_3). Thus, *arc*+ neurons from the extensively paired group did not exhibit the synaptic enhancement up to 3 days after training, and only developed a substantial synaptic enhancement on the 5th day.

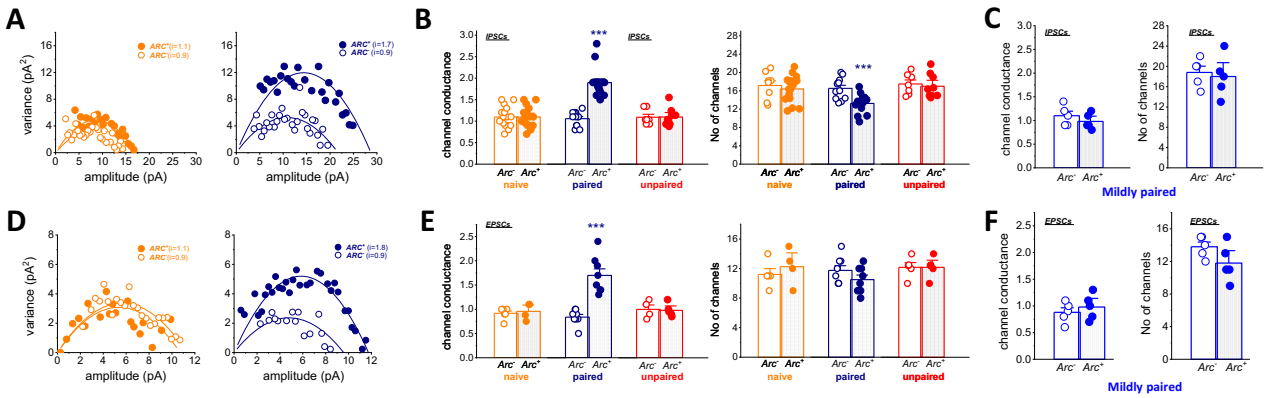

Fig. 2 | Enhanced synaptic strength is mediated by increase in synaptic channel conductance. A, **D** Current variance plot extracted from the peak scaled mIPSCs (**A**) and mEPSCs (**D**) from *arc*+ and *arc*− neurons of the extensively paired training animals (blue) and naïve animals (orange). The larger initial slope in the *arc*+ cells from the extensively paired group, indicates that the current mediated by a single synaptic channel is larger. **B**, **E** The single synaptic channel current (left), but not the number of channels (right) of *arc*+ neurons from the extensively paired group is larger than *arc*− neurons and neurons from the control groups (naïve, unpaired) for inhibition (**B**) and excitation (**E**). Each point represents the single-channel current (**B**, **E**, left) or the number of channels (**B**, **E**, right) in a single cell. **C**, **F** The single synaptic channel current (left) and the number of channels mediating an averaged synaptic event for *arc*+ *and arc*− neurons from the mildly trained group for inhibition (**C**) and excitation (**F**). Each point represents the single-channel current (**C**, **F**, left) or the number of channels (**C**, **F**, right) in a single cell. Statistics (**B**–**F**): Bars represent mean ± SE. (*P < 0.05; ***P < 0.001). Two-way ANOVA: single-channel current for inhibition: *arc* +/*arc* −: $F_{1,65}$ = 18.4; $p = 5.9 \times 10^{-5}$. Groups (naïve, unpaired, extensively paired, mildly paired): $F_{3,65}$ = 17.6; $p = 1.7 \times 10^{-8}$. Interaction: $F_{3,65}$ = 24.2; $P = 1.2 \times 10^{-10}$. Single-channel current for excitation: *arc* +/*arc* −: $F_{1,35}$ = 27.1; $p = 8.5 \times 10^{-6}$. Groups (naïve, unpaired, extensively paired, mildly paired): $F_{3,35}$ = 7.6; P = 0.0005. Interaction: $F_{3,35}$ = 10.7; $p = 3.8 \times 10^{-5}$.

https://doi.org/10.1038/s41467-025-64854-5

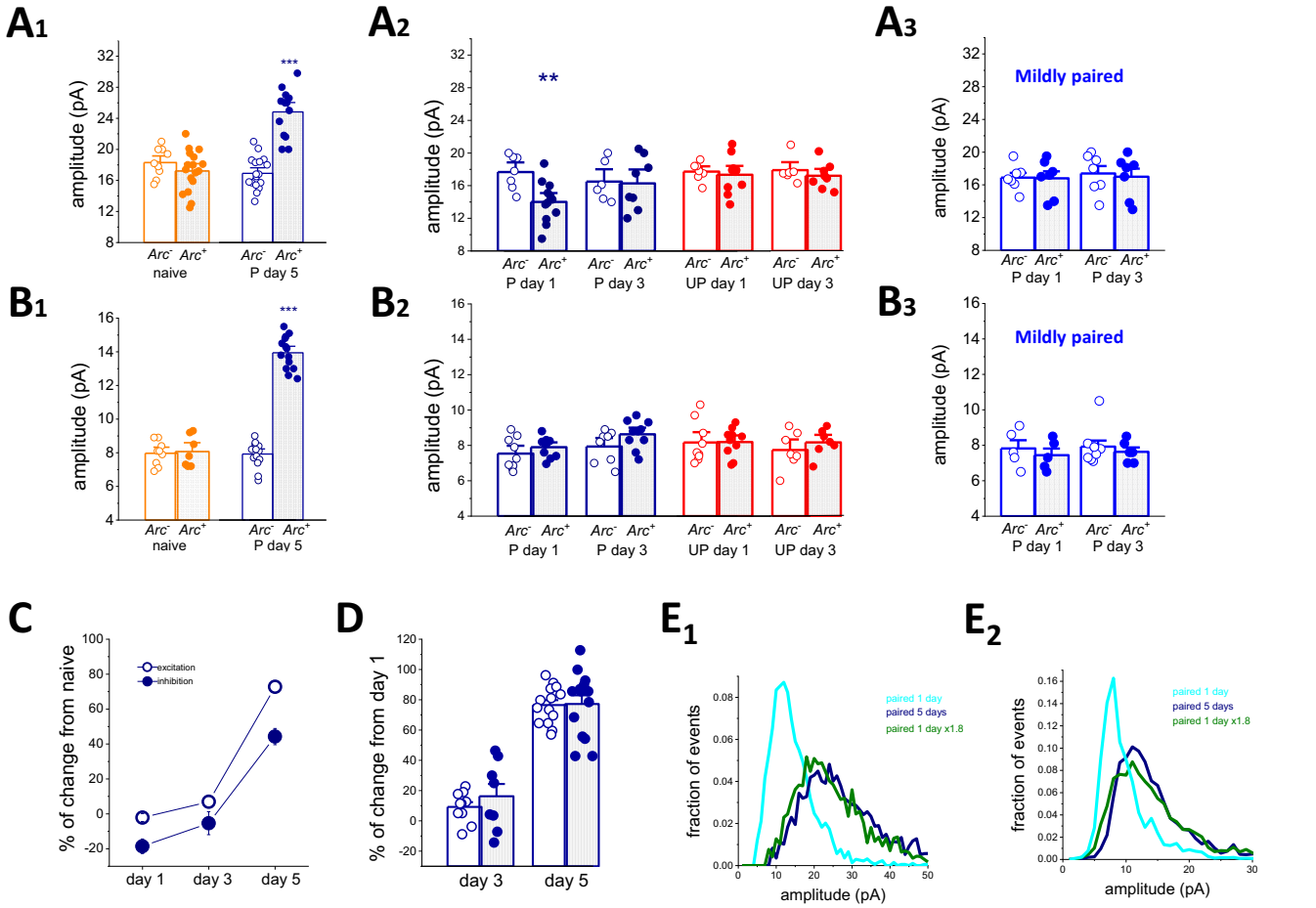

Fig. 3 | The time courses of enhanced inhibition and excitation are similar and only emerge 5 days after training completion. A_1, B_1. Values from the naïve and extensively trained groups 5 days after training for inhibition (A_1) and excitation (B_1). Each point represents the averaged synaptic event amplitude for each neuron. Bars represent mean ± SE. A_2, B_2, A_3, B_3 Miniature inhibitory (A_2) and excitatory (B_2) synaptic events were recorded on the 1st and 3rd days after fear training from *arc*+ and *arc*− neurons from extensively paired (indicated by *P*) and unpaired groups (indicated by UP) as well as from *arc*+ and *arc*− neurons from the mildly paired group (A_3, B_3). One day after training, the averaged inhibitory event amplitude in *arc*+ cells from the extensively paired group was lower than the control groups. Each point represents the value for each neuron. Bars represent mean ± SE. (**$P < 0.01$, ***$P < 0.001$). statistics (A_1, A_2, A_3): Three-way ANOVA: mIPSCs: interaction: day: $F_{1,97} = 4.35$; $P = 0.04$; groups (naïve, unpaired, extensively paired, mildly paired): $F_{1,97} = 2.29$, $P = 0.1$; *arc* + /*arc* −: $F_{1,97} = 2.17$; $P = 0.14$; interaction: $F_{3,97} = 3.7$; $P = 0.028$. mEPSCs: interaction: $F_{3,83} = 0.06$; $p = 0.94$. **C** The averaged synaptic event amplitude recorded from *arc*+ cells from the extensively paired group exhibited a sharp rise on the 5th day, both for excitation and inhibition. Each point represents the percentage change in *arc*+ cells from the extensively paired group relative to *arc*+ cells from the naïve group. Bars represent mean ± SE. **D** The modulation in the amplitudes of the synaptic events on day 3 and day 5 was similar and parallel for inhibition and excitation. Each point represents the percentage change in the averaged amplitude of synaptic events recorded from *arc*+ cells on the 3rd and 5th days from the extensively paired group relative to *arc*+ cells recorded on the 1st day after training. Bars represent mean ± SE. E_1, E_2 Mean distribution curves of amplitudes of inhibitory (E_1) and excitatory (E_2) synaptic events in *arc*+ neurons taken from extensively trained mice 5 days after training (blue) and 1 day after training (cyan). The amplitude distribution curve of the *arc*+ cells from the extensively trained group 5 days after training (green) could be reconstructed ($P = 0.88$ for synaptic inhibition and excitation) by multiplying all events in the cells recorded on the 1st day after training by a factor of 1.8 (blue).

The enhancement of synaptic inhibition and excitation is parallel in both magnitude and time course

The time course of change in the mIPSC and mEPSCs amplitude in *arc*+ neurons is summarized in Fig. 3C, where the mean values of *arc*+ cells from the extensively paired group were compared to the mean values of *arc*+ cells from naïve group. For synaptic inhibition, after an initial significant reduction ($P = 0.0026$) of 18.6% in synaptic inhibition 1 day after learning, 3 days after learning the mean value returned to control values (−5.4%, $P = 0.45$) and 5 days after learning a sharp and pronounced increase (41.9%, $P < 0.001$, $n = 8$) was observed.

For synaptic excitation, 1 day and 3 days after training the mean values in *arc*+ neurons taken from extensively trained mice were similar to their counterparts in naïve mice (1 day: 2.1%, $P = 0.64$; 3 days: 6.9%, $P = 0.2$), whereas 5 days after learning a substantial increase was observed (81.2%, $P < 0.001$, $n = 10$).

Interestingly, 2–5 days after extensive fear conditioning, the time course of enhancement of the inhibitory and excitatory synaptic inputs is very similar (Fig. 3D); 3 days after training, synaptic inhibition is enhanced by 16.3% ± 22.9 ($n = 8$) and synaptic excitation by 9.3% ± 10.2 ($n = 10$). These values do not differ significantly ($P = 0.39$). Five days after learning, synaptic inhibition is enhanced by 77.3% ± 21.4 ($n = 14$) and synaptic excitation by 76.5% ± 12.3 ($n = 14$). These two values are practically identical ($P = 0.92$).

The equal magnitude of the increased synaptic strength for inhibition and excitation is in line with the amplification mechanism hypothesis. Moreover, the equivalent time course of the enhancement in synaptic strength indicates that the enhancement of inhibition and excitation is coupled and may be induced by a common mechanism.

The enhanced synaptic strength can be explained as uniform scaling of the strength of all synapses in the arc+ cells

Next, we asked whether the profound enhancement of synaptic strength observed in active neurons after extensive training can be explained by a uniform enhancement of the strength of all synaptic connection, as predicted by the whole-cell amplification mechanism[19]. The increase in averaged inhibitory excitatory event amplitude from the 1st day to the 5th day was similar and amounted to an 80% increase. If learning multiplied the strength of all synapses by the same factor, it should be apparent that the strength of each inhibitory synapse and each excitatory synapse was multiplied by a factor of approximately 1.8. We compared the mean amplitude distribution curves of inhibitory and excitatory mPSCs events in *arc*+ neurons taken from extensively trained mice in three different conditions: 1 day after learning, 5 days after learning and 1 day after learning where all values were multiplied by a factor of 1.8, the mean increase in synaptic strength. For synaptic inhibition, the distribution curves of events 1 day and 5 days after learning were significantly different ($P = 0.019$). After scaling all the events recorded 1 day after training by a factor of 1.8, the two curves almost coincide ($P = 0.88$) (Fig. 3E$_1$). A similar result was obtained for synaptic excitation. The distribution curves of excitatory events 1 day and 5 days after learning were significantly different ($P = 0.018$). Here too, after scaling all events by a factor of 1.8, the two curves almost coincide ($P = 0.88$) (Fig. 3E$_2$). The shape of the distribution curve is highly susceptible to the exact process that underlies its formation[19]. Therefore, the accurate reconstruction of the distribution curve, as shown above, strongly supports the notion that multiplication by a factor of 1.8 of the strength of all synapses underlies the increase in synaptic strength.

Thus, long-lasting enhanced synaptic strength induced by extensive fear conditioning has several unique traits: (1) It is restricted to *arc* + cells of the extensively paired group. (2) Five days after conditioning, synaptic inhibition and synaptic excitation are enhanced to the same extent. (3) It has a long incubation time, developing only 5 days after training. (4) The substantial development of the synaptic enhancement correlates with a pronounced difference in freezing between the mildly and the extensively trained groups at the 5th day after conditioning and with the persistent freezing response that is apparent in extensively trained mice only. (5) Such delayed-developing synaptic strengthening seems to be mediated by a uniform whole-cell process, rather than by a synapse-specific process and is mediated by enhanced conductance of virtually all inhibitory and excitatory synaptic channels in the *arc*+ cells.

Long-lasting enhancement of synaptic strength induced by extensive fear conditioning is mediated by persistent CaMKII activation

It has been well established that CaMKII-mediated phosphorylation of the AMPA channel in ser831 results in a twofold increase in AMPA channel conductance[23–25], which is similar to the increase in the single channel conductance that we observed here. Additionally, we previously showed that olfactory rule-learning-induced enhancement of synaptic inhibition[26] and excitation[27] are dependent on persistent CaMKII activation. We thus examined whether extensive fear-conditioning-induced enhanced synaptic transmission is also mediated by CaMKII-mediated phosphorylation.

For synaptic inhibition, application of the CaMKII blocker KN93 significantly reduced ($P < 0.001$) the mean mIPSC amplitude in *arc*+ neurons from extensively trained mice 5 days after training from 23.8 ± 3.5 to 14.7 ± 2.3 pA ($n = 5$) (Fig. 4A$_1$). By contrast, KN93 did not reduce the mean amplitude in *arc*− neurons from the same mice (17.2 ± 2.2 before KN93 to 18.1 ± 1.4 pA after KN93 ($n = 6$), $P = 0.08$; $n = 7$ mice). In neurons from naïve mice, KN93 did not reduce the mean amplitude in *arc*+ neurons (17.6 ± 2.1 before KN93 to 18.7 ± 2.5 pA after

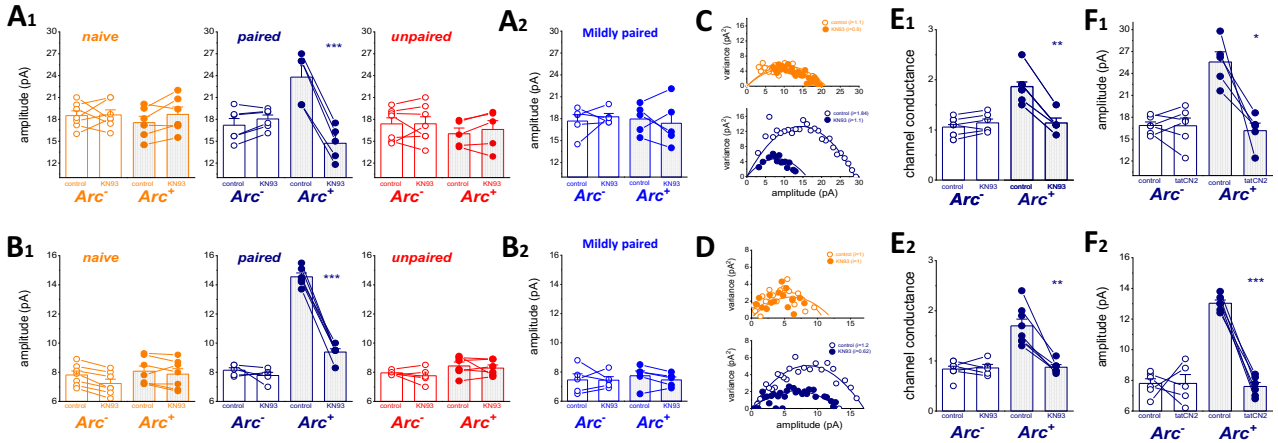

Fig. 4 | CaMKII blocker affects the average synaptic event amplitude selectively in arc+ cells from the extensively trained group. A$_1$, B$_1$. Averaged event amplitudes of inhibitory (**A**) and excitatory (**B**) synaptic events before and after the application of CaMKII blocker (KN93) recorded from *arc*+ and *arc*− neurons from the extensively paired, unpaired and naïve groups (**A1**, **B1**). KN93 had a robust effect on each of the *arc*+ cells from the extensively paired group, both for inhibition (**A$_1$**) and excitation (**B$_1$**). Each point represents the value for each neuron. Bars represent mean ± SE. (***$P < 0.001$). Two-way ANOVA: inhibition: KN93 effect: $F_{1,20} = 2.3$; $P = 0.11$. *arc* + /*arc* − : $F_{1,20} = 16.9$; $P = 0.0005$. Interaction: $F_{1,20} = 20.9$; $P = 0.00018$. Excitation: KN93 effect: $F_{1,18} = 300$; $P = 1.1\times10^{-12}$. *arc* + /*arc* − : $F_{1,18} = 167$; $p = 1.4\times10^{-10}$. interaction: $F_{1,18} = 108$; $P = 4.8\times10^{-9}$. **A$_2$, B$_2$.** KN93 did not affect the mildly trained group for either inhibition (**A$_2$**) or excitation (**B$_2$**). Each point represents the averaged synaptic event amplitude for each neuron. Two-way-ANOVA, $F_{1,16} = 0.36$, $p = 0.5584$. **C**, **D** Current variance plot extracted from the peak scaled mIPSCs (**C**) and mEPSCs (**D**) from *arc* + (blue) and *arc*− neurons (orange) of the extensively trained and naïve animals before and after application of KN93. KN93 affected the single-channel current in *arc*+ cells from the extensively paired group as indicated by the smaller initial slope. **E$_1$, E$_2$.** Single-channel current of *arc*+ neurons from the extensively paired group was largely affected by KN93 both for synaptic inhibition (**E$_1$**) and synaptic excitation (**E$_2$**). Each point represents the value for a single cell. Bars represent mean ± SE. (**$P < 0.01$). Two-way ANOVA: inhibition: KN93 effect: $F_{1,20} = 15.4$; $P = 0.0008$. *arc* + /*arc* − : $F_{1,20} = 11.7$; $P = 0.0027$. Interaction: $F_{1,20} = 17.5$; $P = 0.00046$. Excitation: KN93 effect: $F_{1,18} = 13.6$; $P = 0.0016$. *arc* + /*arc* − : $F_{1,18} = 16.6$; $P = 0.0007$. Interaction: $F_{1,18} = 12.6$; $P = 0.002$. **F$_1$, F$_2$** CaMKII phosphorylation inhibitor tatCN21(5 μM) reduced the averaged amplitude of inhibitory (**F$_1$**) and excitatory (**F$_2$**) miniature synaptic events recorded from *arc*+ neurons from the extensively paired group, but did not affect *arc*− cells from the same group. Each point represents the value for a single cell. Bars represent mean ± SE (*$P < 0.05$; ***$P < 0.001$). Two-way ANOVA: inhibition: tatCN21 effect: $F_{1,18} = 15.7$; $P = 0.0009$. *arc* + /*arc* − : $F_{1,18} = 18.1$; $P = 0.0004$. Interaction: $F_{1,18} = 21.4$; $P = 0.0002$. Excitation: tatCN21 effect: $F_{1,18} = 54$; $P = 7.8\times10^{-7}$. *arc* + /*arc* − : $F_{1,18} = 67$; $P = 1.6\times10^{-7}$. Interaction:$F_{1,18} = 62$; $P = 2.8\times10^{-7}$.

KN93 [$n = 6$], $P = 0.1$) and in *arc*− neurons (18.5 ± 1.7 before KN93 to 18.6 ± 1.8 pA after KN93 [$n = 7$], P = 0.91; $n = 5$ mice). Additionally, in neurons from unpaired mice KN93 did not reduce the mean amplitude in *arc*+ neurons (16.0 ± 1.8 before KN93 to 16.2 ± 2.7 pA after KN93 [$n = 5$], $P = 0.32$) and in *arc*− neurons (17.2 ± 2.2 before KN93 to 18.1 ± 1.4 pA after KN93 [$n = 6$], $P = 0.08$; $n = 5$ mice). In neurons from mildly trained mice, KN93 did not reduce the mean amplitude in *arc*+ neurons (17.9 ± 1.9 before KN93 to 17.4 ± 3.1 pA after KN93 [$n = 5$], $P = 0.64$; Fig. 4A_2) or in *arc*− neurons (17.7 ± 1.9 before KN93 to 18.2 ± 1.0 pA after KN93 [$n = 5$], $p = 0.58$; $n = 6$ mice).

Similar results were obtained for synaptic excitation, application of KN93 in *arc*+ neurons from extensively trained mice 5 days after training significantly reduced ($P < 0.001$) the mean mEPSC amplitude from 14.6 ± 0.7 to 9.4 ± 0.6 pA ($n = 5$) (Fig. 4B_1). KN93 did not reduce the mean amplitude in *arc*− neurons from the same mice (8.1 ± 0.4 before KN93 to 7.8 ± 0.5 pA after KN93 [$n = 5$], $P = 0.32$; $n = 5$ mice). In neurons from naïve mice, KN93 did not reduce the mean amplitude in *arc*+ neurons (8.1 ± 0.9 before KN93 to 7.9 ± 1.0 pA after KN93 [$n = 7$], $P = 0.29$). However, a small but highly significant reduction was observed in *arc*− neurons (8.0 ± 0.7 before KN93 to 7.4 ± 10.7 pA after KN93 [$n = 6$], $P = 0.001$; $n = 4$ mice). In neurons from unpaired mice, KN93 did not reduce the mean amplitude in *arc*+ neurons (8.4 ± 0.7 before KN93 to 8.3 ± 0.6 pA after KN93 [$n = 6$], $P = 0.57$) or in *arc*− neurons (8.0 ± 0.2 before KN93 to 7.8 ± 0.6 pA after KN93 [$n = 5$], $P = 0.4$; $n = 3$ mice). In neurons from mildly trained mice, KN93 did not reduce the mean amplitude in *arc*+ neurons (7.7 ± 0.7 before KN93 to 7.4 ± 0.4 pA after KN93 [$n = 5$], $P = 0.18$) (Fig. 4B_2) or in *arc*− neurons (7.4 ± 0.9 before KN93 to 7.4 ± 0.5 pA after KN93 [$n = 5$], $P = 0.95$; $n = 5$ mice).

Thus, the effect of CaMKII blocker was prominent in all *arc*+ cells from the extensively paired group but was neither apparent in *arc*− cells from the same group nor in the control groups.

Long-lasting CaMKII dependent enhancement of synaptic strength is mediated by CaMKII dependent enhancement of the synaptic channel conductance

Application of the CaMKII blocker to neurons from the extensively paired group reduced the single-channel current of both $GABA_A$ and AMPA channels in *arc*+ neurons only (Fig. 4$E_{1,2}$). For synaptic inhibition, application of KN93 in *arc*+ neurons significantly reduced ($P < 0.01$) the mean single-channel current from 1.88 ± 0.4 to 1.14 ± 0.22 pA ($n = 5$). By contrast, KN93 did not modify the current in *arc*− neurons from the same mice (1.07 ± 0.18 before KN93 to 1.14 ± 0.17 pA after KN93 [$n = 6$], $P = 0.09$). Similar results were obtained for synaptic excitation. Application of KN93 in *arc*+ neurons significantly reduced ($P < 0.01$) the mean single-channel current from 1.67 ± 0.44 to 0.88 ± 0.13 pA ($n = 6$). By contrast, KN93 did not modify the current in *arc*− neurons from the same mice (0.88 ± 0.09 before KN93 to 0.86 ± 0.16 pA after KN93 [$n = 5$], $P = 0.79$).

Repeating the experiments with CaMKII blocker tatCN21 attains similar results

To ensure that these effects are indeed specific to CaMKII, we repeated the experiment in neurons from extensively trained mice with the specific CaMKII peptide inhibitor tatCN21 (Fig. 4$F_{1,2}$). For mIPSCs, in *arc*+ neurons from extensively trained mice, tatCN21 application significantly reduced ($P < 0.05$) the mean mIPSC amplitude from 25.6 ± 3.51 to 16.2 ± 2.3 pA ($n = 5$), but did not modify the mean amplitude in *arc*− neurons from the same mice (16.9 ± 1.2 before tatCN21 to 16.8 ± 2.5 pA after tatCN21 [$n = 6$], $P = 0.97$). For mEPSCs, in *arc*+ neurons from extensively trained mice, tatCN21 application significantly reduced ($P < 0.001$) the mean mEPSC amplitude from 13.0 ± 30.5 to 7.6 ± 0.6 pA ($n = 6$), but did not modify the mean amplitude in *arc*− neurons from the same mice (7.6 ± 1.0.7 before tatCN21 to 7.8 ± 21.3 pA after tatCN21 [$n = 5$], $P = 0.86$). Thus, tatCN21 also showed a robust effect in all *arc*+ cells from the extensively trained group only. Moreover, in line with the notion that the effect of CaMKII blocker was mediated through the effect on the amplification mechanism, it could be computationally reversed assuming a multiplication by 1.8 (Supplementary Fig. 3).

These results suggest that: (1) CaMKII-dependent phosphorylation underlies the learning-induced increase in synaptic channel current, for both inhibition and excitation. (2) Virtually all cells that compose the fear engram exhibited CaMKII-dependent increase of the synaptic channel conductance, where it was lacking the non-engram cells. (3) CaMKII mediates both the increase in synaptic inhibition and synaptic excitation, indicating that these modifications are coupled and mediated by the same mechanism. (4) The effect of CaMKII could be computationally reversed assuming a process where the events amplitude was scaled by a factor of 1.8.

Extensive learning induces a calcineurin-dependent long-lasting reduction in the strength of synaptic inhibition in arc+ cells

Next, we aimed to characterize the mechanism that underlies the decreased inhibition strength in cells composing the fear engram 1 day after training (Fig. 3A_2). It was previously shown that neuronal activity reduces the number of $GABA_A$ receptors through a calcineurin-dependent process that increases the diffusion coefficient of the $GABA_A$ channels[28]. Accordingly, we found that extensive fear conditioning induced reduction in synaptic inhibition is dependent on persistent calcineurin activation (Fig. 5A). Application of the calcineurin blocker cyclosporine in *arc*+ neurons from extensively trained mice, 1 day after training, significantly increased ($P < 0.001$) the mean mIPSC amplitude from 14.7 ± 1.6 to 17.9 ± 1.0 pA ($n = 7$). By contrast, cyclosporine did not modify the mean amplitude in *arc*− neurons from the same mice (17.7 ± 1.3 before cyclosporine to 17.3 ± 1.7 pA after cyclosporine [$n = 8$], $P = 0.52$, $n = 6$ mice). In neurons from naïve mice, cyclosporine did not change the mean amplitude in *arc*+ neurons (17.3 ± 1.3 before cyclosporine to 17.5 ± 2.1 pA after cyclosporine [$n = 6$], $P = 0.7$, $n = 4$ mice) or in *arc*− neurons (18.2 ± 2.7 before cyclosporine to 17.3 ± 2.1 pA after cyclosporine [$n = 5$], $P = 0.4$). Similarly, in neurons from unpaired mice, cyclosporine did not change the mean amplitude in *arc*+ neurons (17.6 ± 1.2 before cyclosporine to 17.7 ± 2.1 pA after cyclosporine [$n = 7$], $P = 0.86$, $n = 3$ mice) or in *arc*− neurons (18.2 ± 1.8 before cyclosporine to 18.1 ± 1.9 pA after cyclosporine [$n = 8$], $P = 0.87$).

As shown in Fig. 5B, the cyclosporine-induced enhancement of the mIPSCs is not due to increased single-channel current (1.1 ± 0.1 pA before cyclosporine and 1.1 ± 0.2 pA after [$n = 6$], $P = 0.74$), but due to a significant ($P < 0.05$) increase in the average number of channels that mediates a mean inhibitory event (18.1 ± 4.5 before cyclosporine and 22.3 ± 3.5 after [$n = 6$]).

This calcineurin-dependent mIPSC reduction after extensive fear conditioning is persistent, and apparent 5 days after training (Fig. 5C). At this time point, application of cyclosporine significantly increased ($P < 0.01$) the mean mIPSC amplitude in *arc*+ neurons from 24.8 ± 1.6 pA to 28.6 ± 2.0 pA ($n = 7$). Cyclosporine did not modify the mean amplitude in *arc*− neurons from the same mice (17.6 ± 1.0 before cyclosporine to 17.6 ± 2.0 after cyclosporine [$n = 6$], $P = 0.94$, $n = 6$ mice).

Thus, 1 day after extensive training completion, when the amplification mechanism is not yet expressed, learning induces a long-lasting calcineurin-dependent reduction of synaptic inhibition in the cells composing the fear engram through a reduction in the number of $GABA_A$ channels.

The proportion of neurons that undergo whole-cell synaptic enhancement can be calculated based on recordings in slices from wild-type mice

An estimation of the proportion of neurons that are activated when the crucial fear engram is evoked 5 days after training can be obtained by recording samples of neurons from extensively trained wild-type mice.

https://doi.org/10.1038/s41467-025-64854-5

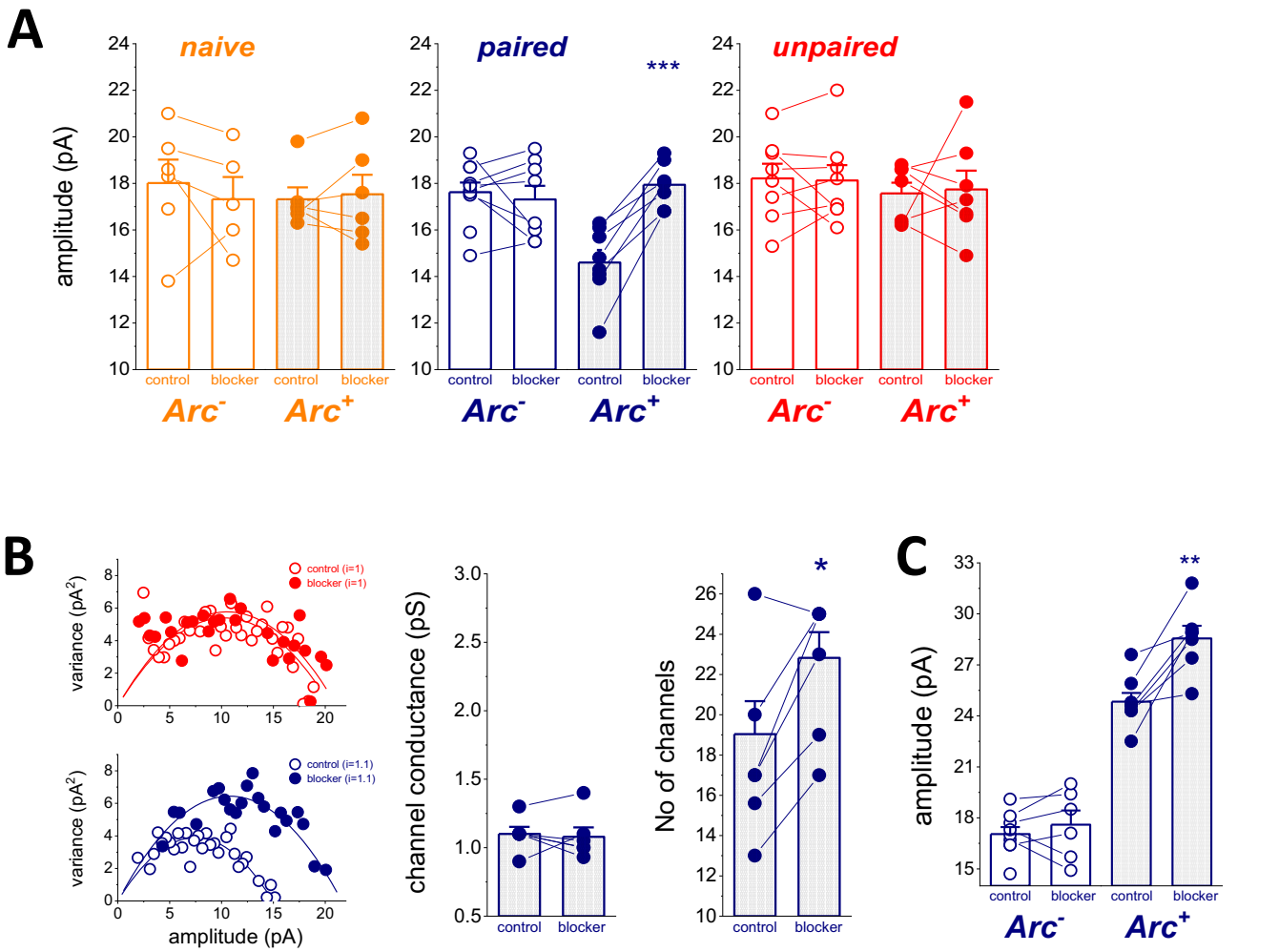

Fig. 5 | Extensive learning induces a calcineurin-dependent long-lasting reduction in the strength of synaptic inhibition in the arc+ cells. A The calcineurin blocker cyclosporine induced an increase in the averaged miniatured inhibitory synaptic events recorded from *arc*+ neurons from the extensively trained group 1 day after training. Each point represents the averaged inhibitory synaptic event amplitude in a single cell. Bars represent mean ± SE. (***$P < 0.001$). Two-way ANOVA: cyclosporine effect: $F_{1,26} = 4.4$, $P = 0.045$; *arc* + /*arc* − : $F_{1,26} = 6.7$, $P = 0.015$; interaction: $F_{1,26} = 12.5$, $P = 0.0015$. **B** Left: Current variance plots demonstrating the effect of cyclosporine on *arc*+ cells from the extensively trained group (blue) and *arc*+ cells from the unpaired group (red). The effect of cyclosporine in *arc*+ cells from the paired group was not mediated through $GABA_A$ single-channel current as indicated by the similar initial slope. Middle: Each point represents the single $GABA_A$ channel current in a single *arc*+ cell from the extensively paired group before and after cyclosporine. Statistics: 2-sides-paired t-test; $T_4 = 0.2$; $P = 0.85$ Right: Cyclosporine induced an increase in the mean number of $GABA_A$ channels mediating miniature inhibitory synaptic events. Each point represents the number of $GABA_A$ channels in a single *arc*+ cell from the paired group before and after cyclosporine. Statistic: two-tailed-paired t-test; $T_4 = 2.93$; $P = 0.42$. Bars represent mean ± SE. (*$P < 0.05$). **C** The effect of cyclosporine on the averaged amplitude of inhibitory synaptic events recorded from *arc*+ neurons from the extensively paired group was also maintained 5 days after training completion. Each point represents the averaged inhibitory synaptic event amplitude in a single cell. Bars represent mean ± SE. (**$P < 0.01$). Two-way ANOVA: cyclosporine effect: $F_{1,18} = 144$, $P = 4.8 \times 10^{-10}$; *arc* + /*arc* − : $F_{1,18} = 10.2$, $P = 0.0049$; interaction: $F_{1,18} = 5.86$, $P = 0.026$.

In slices taken from wild-type mice, "engram" neurons cannot be distinguished visually from "non-engram" neurons and thus our measurements are averages across the population.

Our data show that when recording under these conditions, the average of both mIPSCs and mEPSCs are higher in neurons from extensively paired mice 5 days after training (Fig. 6A, B, D). The mean amplitude of inhibitory events in neurons from extensively paired mice (Fig. 6A) (20.4 ± 5.3 pA, $n = 28$) was significantly ($F_{2,66} = 6.12$, $P = 0.0037$, $n = 8$ mice) higher than the mean amplitude in neurons from naïve (16.3 ± 3.9, $t = 2.63$, $P = 0.0065$, $n = 15$, $n = 5$ mice), unpaired mice (17.1 ± 2.4, $t = 2.71$, $P = 0.0093$, $n = 23$, $n = 4$ mice) and mildly trained mice (17.0 ± 1.8, $t = 2.7$, $P = 0.011$, $n = 7$, $n = 4$ mice) (Fig. 6D). The mean values of the naïve mice, the unpaired group and the mildly trained group did not differ ($F_{2,45} = 0.42$, $P = 0.662$, Fig. 6A, D) and were similar to the control values obtained from *arc::dVenus* mice (paired *arc* − 16.9 ± 2; unpaired *arc* + 17.3 ± 2.9; naïve *arc* + 17.2 ± 2.6; mildly trained *arc* + 16.1 ± 3.1 pA).

The mean amplitude of excitatory events in neurons from extensively paired mice (Fig. 6B) (10.6 ± 3.3 pA, $n = 26$, $n = 8$ mice) was significantly ($F_{2,66} = 10.9$, $P < 0.01$) higher than the mean amplitude in neurons from naïve mice (7.8 ± 1.0, $t = 4.03$, $P = 0.0003$, $n = 21$, $n = 7$ mice), unpaired mice (8.2 ± 1.0, $P = 0.0037$, $n = 19$, $n = 5$ mice) and mildly trained mice (7.0 ± 0.5, $P = 0.000015$, $n = 7$, $n = 3$ mice) (Fig. 6D). The mean values of the naïve mice, the unpaired group and the mildly paired group did not differ ($P = 0.28$; Fig. 6B, C), and were similar to the control values obtained from *arc::dVenus* mice (paired *arc* − 7.9 ± 0.8; unpaired arc+ 8.4 ± 0.7; naïve *arc* + 8.1 ± 0.9; mildly paired *arc* + 8.2 ± 1.6). The average increase in synaptic inhibition (percent change from naïve) was 25.3% ± 32.7 and in synaptic excitation 35.0% ± 42.0. These values did not differ significantly ($P = 0.35$; Fig. 6C).

https://doi.org/10.1038/s41467-025-64854-5

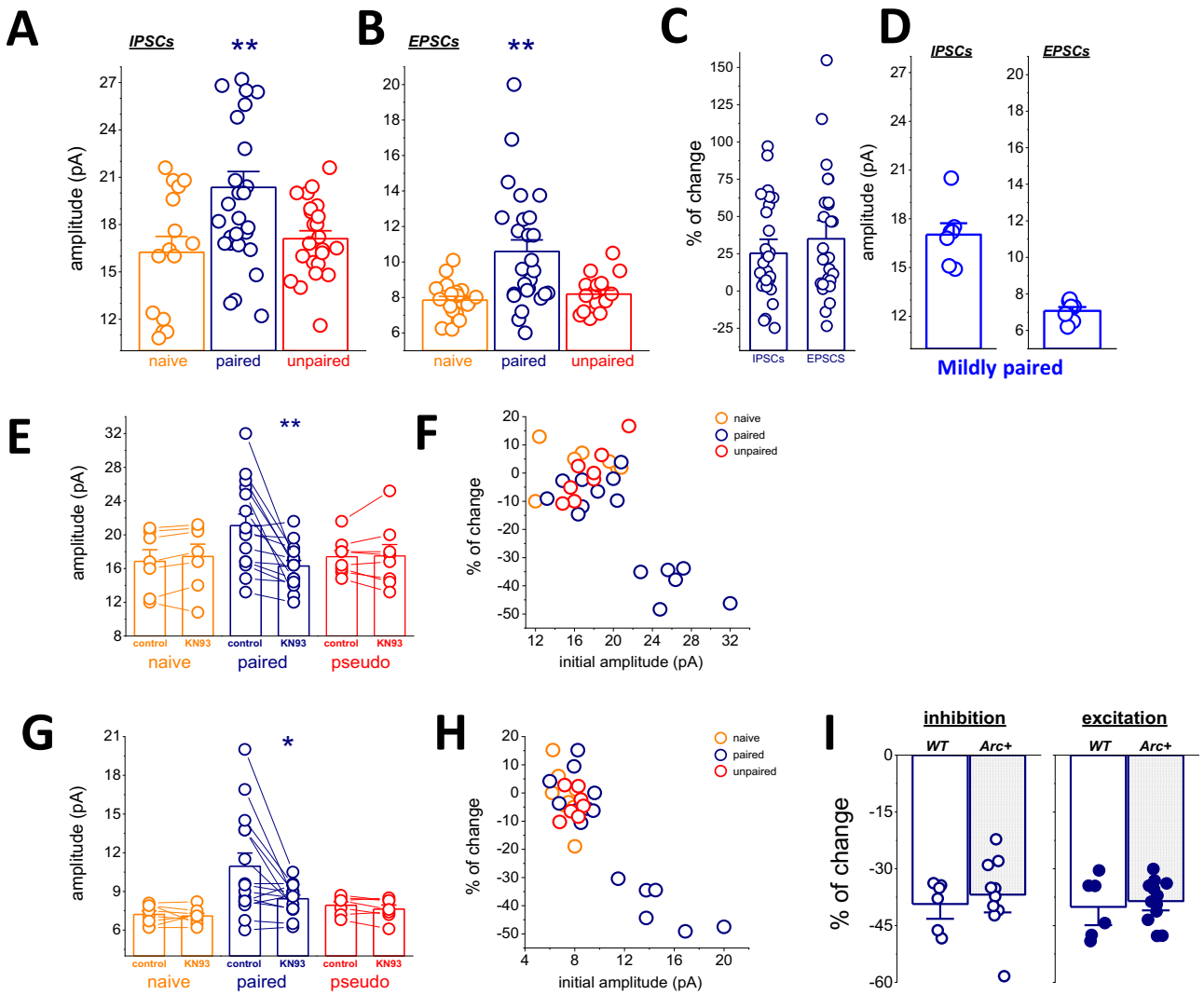

Fig. 6 | The training-induced enhancement in the synaptic strength is also evident in the wild-type group. A, **B** Fear training induced an increase in the amplitudes of inhibitory (**A**) and excitatory (**B**) synaptic events recorded from wild-type mice 5 days after training (mIPSC's: one-way ANOVA, $F_{2,66} = 6.12$, $P = 0.0037$. mEPSC's: one-way ANOVA, $F_{2,62} = 5.4$, $P = 0.0067$). Each point represents the averaged synaptic event amplitude in a single cell. Bars represent mean ± SE. (**$P < 0.01$). **C** The percentage change was similar for synaptic inhibition and synaptic excitation. Each point represents the percentage change relative to the naïve group. Bars represent mean ± SE. add F 's. **D** The mildly trained group exhibited values that are similar to controls both for inhibition and excitation. Each point represents the percentage change relative to the naïve group. Bars represent mean ± SE. **E**, **G** CaMKII blocker KN93 decreased the amplitude of inhibitory (**E**) and excitatory (**G**) synaptic events recorded from the extensively paired group (mIPSC's: two-tailed-paired-ttest, $t_{11} = 3.66$, $P = 0.0026$; nEPSCs: two-tailed-paired-ttest, $t_{10} = 2.82$, $P = 0.0135$). Each point represents the averaged synaptic event amplitude in each neuron. Bars represent mean ± SE. (*$P < 0.05$; **$P < 0.01$). **F**, **H** Each cell was plotted as a function of percentage change induced by KN93 (y axis) and its amplitude before application of KN93 (x axis), yielding a clear clustered effect where the affected cluster exhibited a large CaMKII blocker effect, and the non-affected cluster exhibited no effect for either inhibition (**F**) or excitation (**H**). **I** The effect of KN93 on *arc*+ cells from the extensively trained group of *arc::dVenus* mice (*arc* +) is similar to its effect on the affected cluster from the extensively paired group in the wild-type mice (WT), both for inhibition and excitation. Each point represents the percentage of change induced by KN93 on averaged synaptic event amplitude in each neuron. Bars represent mean ± SE.

Assuming that the increase in events amplitude both for inhibition and excitation is caused by the induction of the amplification mechanism on a fraction of the cells, the fraction of engram cells can be calculated from the averaged amplitude of events in wild-type mice and from the averaged amplitude of synaptic events in *arc*+ and *arc*− neurons.

Thus, if X is the fraction of engram (*arc* +) neurons and $1 - X$ the fraction of neurons that are not part of the engram (*arc*− neurons), then for synaptic inhibition the following calculation can be done: $24.8X + 16.9(1 - X) = 20.4$ (where 24.8 and 16.9 are the averaged event amplitudes recorded from *arc*+ and *arc*− cells, respectively, in the extensively trained group; 20.4 is the averaged event amplitude for wild-type mice from the extensively trained group). For synaptic excitation the calculation is performed similarly: $13.9X + 7.9(1 - X) = 10.6$. These simple equations give X values of 0.44 for synaptic inhibition and 0.45 for synaptic excitation. Thus, calculations for both inhibition and excitation predict that around 45% of the cells belong to the amplified fear engram.

To further examine the validity of these calculations, we examined the effect of KN93 on the mEPSCs and mIPSCs amplitudes in neurons recorded from wild-type mice 5 days after extensive fear conditioning. Based on our findings and the calculations above, we predicted that KN93 should only significantly reduce both IPSCs and EPSCs in approximately 45% of neurons from paired mice.

Application of KN93 significantly reduced the mean mIPSC amplitude in neurons from paired mice from 21.1 ± 5.3 to 16.2 ± 2.6 pA

(($t = 3.66$, $P = 0.0026$) $n = 15$; Fig. 6E). KN93 did not reduce the mean amplitude in neurons from naïve (16.9 ± 3.7 before KN93 to 17.4 ± 3.9 pA after KN93 [$n = 7$], $t = 1.7$, $P = 0.14$) or unpaired mice (17.4 ± 2.1 before KN93 to 17.5 ± 3.8 pA after KN93 [$n = 8$], $t = 0.16$, $P = 0.87$). Moreover, as shown in Fig. 6F, the effect of KN93 was strongly pronounced (39.3 ± 6.4%) in six out of fifteen neurons recorded in the paired group. These neurons, composing 40% of neurons in the paired group, were the six neurons with the highest initial amplitudes.

Almost identical results were obtained for synaptic excitation. Application of KN93 significantly reduced ($t = 2.82$, $P = 0.0135$) the mean mEPSC amplitude in neurons from paired mice from 10.9 ± 4.0 to 8.4 ± 1.2 pA ($n = 15$; Fig. 6G). KN93 did not reduce the mean amplitude in neurons from naïve (7.2 ± 0.8 before KN93 to 7.1 ± 0.6 pA after KN93 [$n = 8$], $t = 0.36$, $P = 0.73$) or unpaired mice (7.9 ± 0.7 before KN93 to 7.6 ± 0.8 pA after KN93 [$n = 7$], $t = 2.07$, $P = 0.08$). Here too (Fig. 6H), the effect of KN93 was strongly pronounced in six out of fifteen neurons recorded in the paired group (40.1 ± 7.8%) and exactly as shown for synaptic inhibition, this profound effect appeared on 40% of neurons in the paired group, which were the six neurons with the highest initial amplitudes.

This measured fraction of CaMKII-affected cells both for inhibition and excitation matches the calculation that approximately 40% of the cells participate in the amplified fear engram. Moreover, these results are in line with other studies that measured the fraction of active cells during cued fear conditioning using immunohistochemistry methods[29].

The synaptic characteristics of the CaMKII-affected cells from wild-type mice and arc+ cells from arc::dVenus mice are equivalent

Five days after extensive conditioning the CaMKII-affected cells from wild-type mice were practically equal in all parameters to the *arc*+ cells from *arc::dVenus* mice both for synaptic inhibition and synaptic excitation (Table 2). Moreover, the amplitude distribution curves of these two groups were practically identical (Supplementary Fig. 4), indicating that the CaMKII affected cells are likely to be the subset of cells that compose the fear engrams, and that the amplification mechanism was induced on these cells.

The great similarity between the CaMKII-affected neurons from wild-type mice and the *arc*+ neurons from *arc::dvenus* mice is also evident when quantitatively comparing the effect of the CaMKII blockers on the amplitudes of both mIPSCs and mEPSCs in these cells (Fig. 6I). For synaptic inhibition, in CaMKII-affected neurons, CaMKII blocker reduced the averaged amplitude by 39.3% ± 6.4 ($n = 6$) and in *arc*+ neurons by 36.8% ± 9.9 ($n = 10$). These values do not differ statistically ($P = 0.59$). For synaptic excitation in wild-type neurons the CaMKII blocker reduced the mean amplitude by 40.1% ± 7.8 ($n = 6$) and in *arc*+ neurons by 38.5% ± 5.7 ($n = 12$). These values also do not differ statistically ($P = 0.63$).

The equal effect of CaMKII blocker on both synaptic inhibition and synaptic excitation in both wild-type and *arc::dvenus* mice is a direct consequence of the learning-induced uniform effect on the strength of all inhibitory and excitatory synapses in the neuron. Such a uniform process is likely to result in repeatable and identical modifications of the synaptic characteristics of the engram cells. Moreover, assuming that the strength of all synapses was multiplied by a factor of 1.8 (Fig. 3), the calculated effect of CaMKII blocker should be a reduction of 44% ((1.8 − 1)/1.8), a value that is similar to the experimental effect of CaMKII blocker.

Moreover, the wild-type mice did not undergo a fear retrieval on the 5th day after training, indicating that the training itself was sufficient to trigger a process in which 5 days later the amplification mechanism was selectively induced on cells composing the fear engram. This observation validates the concept of engram amplification, which differs from engram formation and engram reconsolidation.

Next, we aimed to explore the computational aspects of such a process where the strength of all the inhibitory and excitatory neurons is doubled in a group of cells that compose an engram.

Computational study. Next, we used network simulations and a mean-field solution of attractor networks to examine whether induction of the amplification mechanism on each of cells that compose an engram, functions as an engram amplification mechanism. An engram is defined by the subset of cells that compose it and by the external input (cue) that activates it. Therefore, an engram amplification mechanism should amplify the engram response while preserving its cell composition and the specificity of the input that activates it. Moreover, an engram amplification mechanism should have an additional effect on the reverberations between engram cells, allowing a greater effect on a learned engram. This requires that (1) upon engram activation the amplification mechanism should selectively increase the firing activity in all neurons composing the engram. (2) The same subset of cells should respond to the external input before and after the amplification mechanism was induced. (3) Accordingly, if the engram is not evoked by the external input, it should also remain silent after the induction of the amplification mechanism. (4) The amplification should have a larger effect on a learned engram through increasing the reverberation between the participating neurons.

Network simulations

Description of simulations. During a Hebbian learning session, a randomly selected external input was repeatedly applied to the network, resulting in the formation of a learned neuronal ensemble. Subsequently, the ensemble was retrieved by applying the same

Table 2 | comparison of different parameters (raw headers) of synaptic events recorded from *arc*+ cells from extensively paired *arc::dvenus* mice and CaMKII sensitive cells from extensively trained wildtype mice

Synaptic inhibition	Paired *arc* +	Paired CaMKII affected	*P* value
Averaged amplitude IPSCS	24.8 ± 2.9 ($n = 14$)	26.5 ± 3.1 ($n = 7$)	0.9
$GABA_A$ single channel current	1.9 ± 0.33 ($n = 8$)	2.00 ± 0.31 ($n = 7$)	0.55
# $GABA_A$ channels	15.9 ± 2.8 ($n = 8$)	16 ± 3.4 ($n = 7$)	0.8
Percent change amp IPSCS	36.8 ± 9.9 ($n = 5$)	39.3 ± 6.4 ($n = 7$)	0.59
Percent change $GABA_A$ single channel current	40 ± 5 ($n = 5$)	44 ± 17 ($n = 7$)	0.9
Synaptic excitation			
Averaged amplitude EPSCS	13.9 ± 1.0 ($n = 14$)	14.8 ± 2.83 ($n = 7$)	0.55
AMPA single channel current	1.7 ± 0.38 ($n = 8$)	1.5 ± 0.08 ($n = 6$)	0.26
# AMPA channels	10.5 ± 1.7 ($n = 8$)	11.9 ± 1.1 ($n = 6$)	0.14
Percent change amp EPSCS	38.5 ± 5.7 ($n = 6$)	40.1 ± 7.8 ($n = 7$)	0.63
Percent change AMPA single channel current	45 ± 9 ($n = 6$)	46 ± 7 ($n = 6$)	0.93

external input, and the cells composing the retrieved ensemble were identified based on their significantly elevated spiking response. The amplification mechanism was implemented by doubling the strength of all inhibitory and excitatory synapses in this responding subset of neurons. This approach enabled a full dissociation between the engram formation and engram amplification as is evident by the experimental result.

The simulations were performed on an extended parameter space, in which both the structure of the network and the external input were varied. Thus, for each set of network parameters (4 sets in total), 10 different sets of external inputs were applied, which resulted in 10 different ensembles. The network response for each set of inputs was averaged over 15 iterations.

The amplification mechanism amplifies the response of the engram selectively upon retrieval while maintaining its composition. We examined whether the induction of the amplification mechanism on a learned ensemble increases the mean firing rate of the retrieved ensemble. For all ensembles, induction of the amplification mechanism robustly multiplied the ensemble spiking response where on average it amounted to a multiplication factor of 1.96 ± 0.16 (Fig. 7A). Moreover, the number of spikes was similarly multiplied in all neurons composing the engram (Fig. 7B).

To test whether the amplification maintains the composition of the engram, we measured the correlation between the network activity before and after the amplification of the learned ensemble. The correlation yielded a value of 0.89 ± 0.05 (range, 0.73–0.95; Fig. 7C) indicating that the ensembles composition was essentially preserved, and thus that the same subset of cells responds to the input.

The cells composing the learned engram are reactivated by specific cues associated with the training experience, and therefore, the amplified ensemble should remain silent at rest. The amplification mechanism had a minor effect on the firing rate of the amplified engram during rest ($9 \pm 2\%$, $P < 0.2$). Moreover, the amplification mechanism did not cause a spontaneous retrieval of the engram as there was a low correlation between the network activity at rest and the network activity during engram retrieval (0.12 ± 0.06).

The amplification mechanism has a stronger effect when applied on cells that compose a learned ensemble

We argued that the amplification mechanism should have a larger effect on learned ensembles through increases in the reverberations between the cells in the ensemble. To test this, we implemented a set of simulations in which the memory pattern was not learned. The effect of the amplification mechanism was robustly reduced ($-30 \pm 5\%$, Fig. 7D) in the non-learned memory pattern. We further tested this hypothesis by applying the amplification mechanism on only a quarter of the cells in a learned ensemble. This manipulation reduced the amplification effect on this subset of cells by $-33 \pm 10\%$ ($P < 0.01$, Fig. 7E). These findings are in line with the scaling effect of the amplification mechanism on the momentary fluctuations of the synaptic current.

Together, these results indicate that the amplification mechanism has a larger effect on a learned engram.

Amplification of the ensemble response increases its statistical strength. The spiking response to the same behavioral stimuli tends to vary widely between iterations and thus a stable neuronal response is typically calculated by averaging over a number of iterations. We reasoned that the increased response of the cells composing the ensemble will decrease its sensitivity to external and internal noise.

The sensitivity of the engram to noise can be measured by the number of iterations that the network activity needs to be averaged over to yield a consistent representation of the network response. We found that the activity of the amplified engram in a single iteration only resembled stable activity when averaged over 15 iterations, yielding a correlation of 0.75 (Fig. 7G). However, if the engram was not amplified, a correlation value of 0.75 was attained only after averaging over seven iterations. Thus, the amplified engram appears to be less noise sensitive and highly reproducible between iterations.

We concluded that applying the amplification mechanism to cells that compose a neural ensemble doubles the average number of spikes emitted by the ensemble, while preserving its composition. Moreover, the engram amplification mechanism did not cause spontaneous retrieval of the ensemble; it had a stronger effect on a learned memory and it robustly increased the statistical power of the ensemble.

Attractor simulations. Attractor networks serve as a key theoretical model to establish the properties of Hebbian-formed memory systems where the memory maintains its activity also in the absence of an external input. The associative connections between neurons enables the resulting reverberations between the memory cells to maintain active memory in the absence of external input. We studied whether the induction of the amplification mechanism on the memory cells can promote the memory into a stable memory through boosting the reverberations between the neurons and if the input selectivity is maintained also after the amplification. We implemented a previously published realistic model of attractor networks of firing neurons, where the neurons are described by their firing rates[30] (see "Methods"). The network was modified to allow the implementation of the memory amplification mechanism.

Here, we provide a general description of the network; for more detail, refer to the original work[30] and the methods section. The network consists of two pools of inhibitory and excitatory spiking neurons that maintain the inhibition–excitation balance. Random ensembles are stored according to the Hebbian learning rule, where β scales the Hebbianic-formed excitatory connections. When β is too low, and thus the associative connection between the cells in the ensemble is too weak, the memory is not retrieved and the subpopulations fire at the same rate as the background. As β increases a new pair of equilibria appears. Of these, the one at the higher firing rate is stable, indicating that a stable memory can be retrieved.

Induction of memory amplification mechanism. The uniform two-fold increase of the strength of all inhibitory and excitatory synapses in the cell enables the implementation of the amplification mechanism simply through modification of the gain function, which calculates the number of spikes given the summation of all synaptic inputs to the cell. More specifically, at each point in time and for each of the attractor neurons the net synaptic current, which is the summation of all the inhibitory and excitatory synaptic currents in the cell, was multiplied by two.

We explored a wide parameter space where we systematically varied the strength of the external inputs, the background connection strength between the neurons, the fraction of neurons that participated in the memory and the strength of synaptic coupling between cells in the memory. This systematic variation of the parameters enables us to compare the effect of the amplification mechanism to the effect of the other parameters.

The amplification mechanism can promote a learned memory into a stable memory by increasing the reverberations between memory cells. Multiplication of the net synaptic current is equivalent to increasing the steepness of the gain function. Such modulation of all neurons composing the memory can amplify the reverberations between them and thus promote a non-stable memory into a stable memory.

We found that if the coupling between cells was rather low, and just too low to sustain a stable memory, the induction of the

https://doi.org/10.1038/s41467-025-64854-5

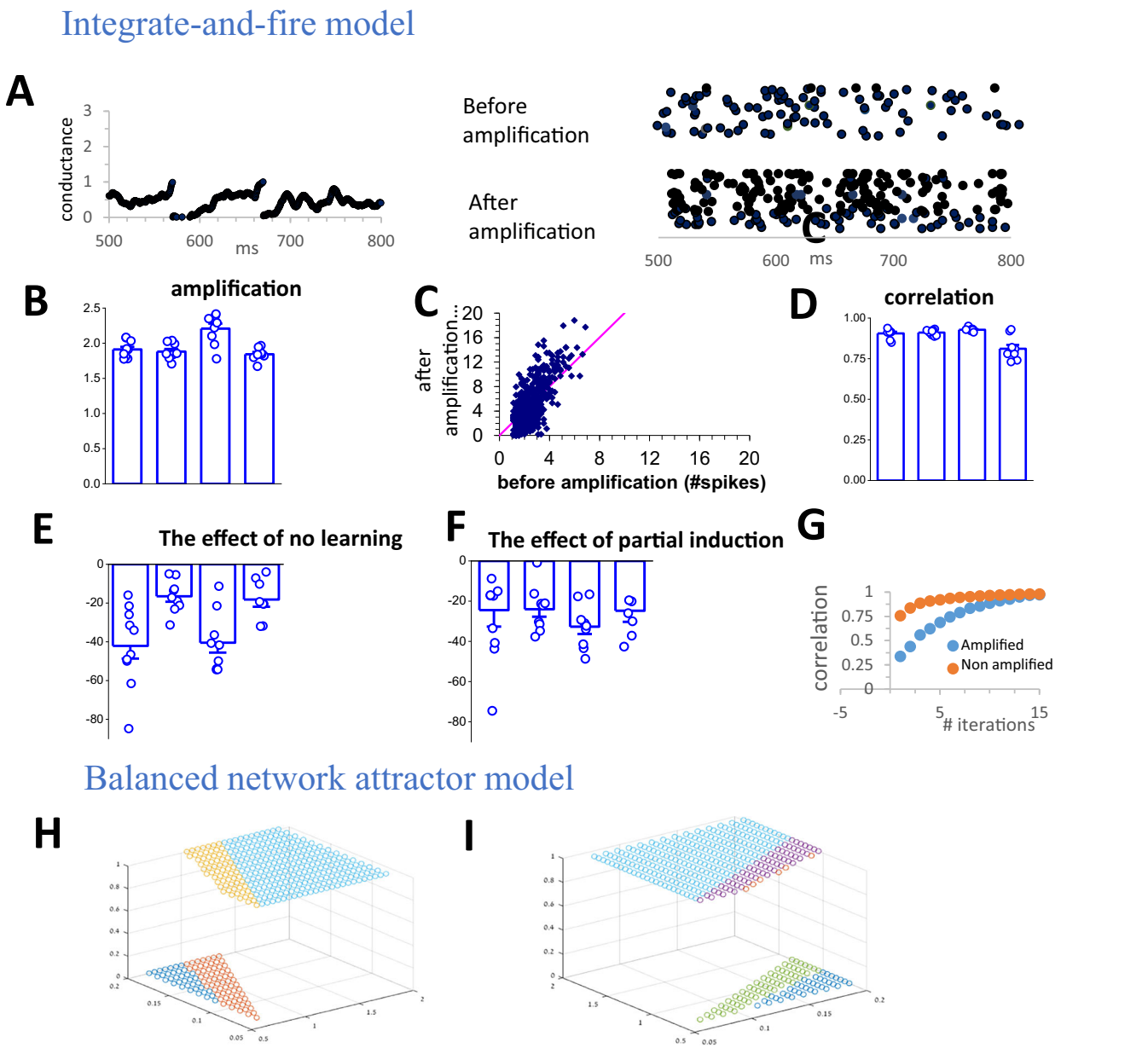

Fig. 7 | Twofold increase of the strength of all synapses in all the cells composing the engram satisfies all the requirements from an engram amplification mechanism. A Left: The cell fires when the conductance reaches the value of one, where thereafter the conductance is reset to zero. Right: Spike raster plot of the neurons participating in the ensemble before and after the amplification. **B** The gain induced by the amplification mechanism on the average number of spikes emitted by the ensemble. Each bar denotes simulations that were performed with different network parameters. Each point is the number of spikes for one simulation. Bars represent mean ± SE. **C** The number of spikes in each ensemble cell before (*x*-axis) and after (*y*-axis) memory amplification. Cells were collected from all simulations. **D** The correlation between the network activity before and after the induction of memory amplification mechanism. Each bar represents a different set of network parameters. Each point is the correlation for one simulation. Bars represent mean ± SE. **E** The amplification yields a smaller effect when induced on a non-learned ensemble. Calculated as the reduction in the amplification of the non-learned ensemble compared with the learned ensemble. Each point represents the value for one simulation. Bars represent mean ± SE. **F** The amplification mechanism yields a smaller effect when induced on a randomly selected 25% of the cells. Each point represents the value for one simulation. Bars represent mean ± SE. **G** Correlation between the network responses averaged over 15 iterations and the network activity averaged over less than 15 iterations. **H** If β is too weak to enable a stable-memory (red, $Z = 0$) the amplification mechanism promoted it into a stable memory (orange, $Z = 1$). Existence of stable memory retrieval (*z*-axis); β (*x*-axis); percentage of memory cells (*y*-axis). **I** Comparison between the effect of memory amplification and the effect of increasing β by 30%. At low levels of β (dark-blue), neither memory amplification nor increasing β by 30% could not promote the memory into a stable memory (dark-blue, $Z = 0$). At intermediate levels of β (green) both memory amplification and increasing β by 30% promoted the memory into a stable memory (purple, $Z = 0$). Red: Memory amplification but not increasing β by 30% promoted the memory into a stable memory (blue, $Z = 1$).

amplification mechanism promoted the memory into a stable memory (Fig. 7G). The effect of the amplification mechanism could be quantified by comparing it to the effect of increasing the strength of the associative coupling. We found that the effect of the amplification mechanism was equivalent to a 30% increase of the coupling between cells (Fig. 7H, in 92% of the simulations both modulations could independently promote a stable memory). Thus, although the effect of the amplification mechanism is cell specific, its effect goes beyond the single-cell level, where it helps to stabilize a memory through increasing the reverberation between memory cells.

https://doi.org/10.1038/s41467-025-64854-5

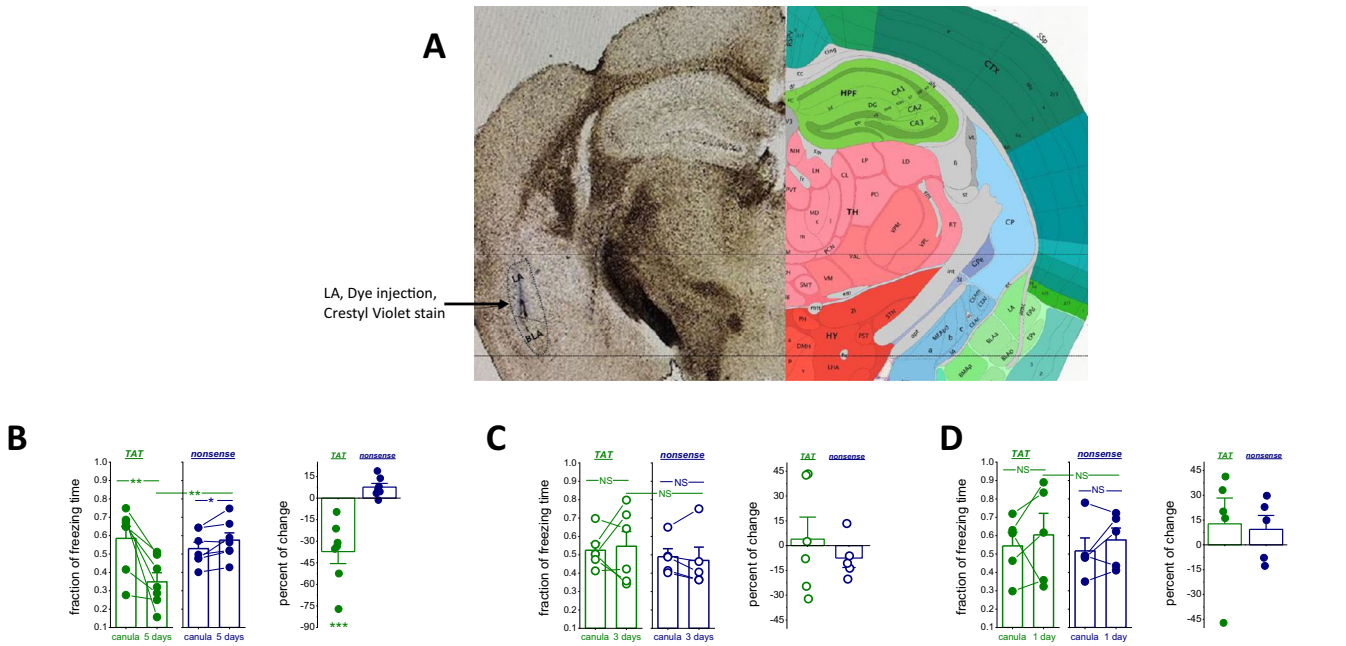

Fig. 8 | Blocking CaMKII results in reduction of freezing response 5 days after training. A Stereotaxic surgery and dye injection for LA coordinates. Picture showing a coronal brain slice of the LA (in purple) from a mouse injected with Cresyl violet stain through the implanted guide cannula (left image) and the corresponding mouse brain atlas (right image). Coronal Image adapted from the Allen Mouse Brain Atlas (© Allen Institute for Brain Science, 2025; available at https://mouse.brain-map.org). **B** CaMKII blocker (tatCN21, 1.5 μg/μl, green) or its control nonsense peptide (tatCtr, 1.5 μg/μl, blue) was injected into the LA through the cannula on the 5th day after training. Injection of tatCN21 2 hours before the retrieval on the 5th day reduced the freezing response (indicated as '5 days') as compared with the freezing response when tatCtr was injected (two-tailed-ttest $T_{13} = 3.55$, $P = 0.0039$), and as compared with the freezing response on the 1st day after training (indicated as 'cannula') when no drug was injected. Each point represents the fraction of freezing response in each mouse. Bars represent mean ± SE. (*$P < 0.05$; **$P < 0.01$). **C** Application of tatCN21 and tatCtr on the 3rd day after learning, before engram amplification was induced, did not affect the freezing response (two-tailed-ttest, $t_6 = 0.48$, $P = 0.64$). Each point represents the fraction of freezing response in each mouse. Bars represent mean ± SE. **D** tatCN21 or tatCtr were injected at the end of training (on the retrieval after 2 days of fear conditioning) and 1 day after training (1 day later, Supplementary Fig. 5). tatCN21 did not modify the freezing response (two-tailed-ttest, $t_9 = 0.21$, $P = 0.84$). Each point represents the fraction of freezing response in each mouse. Bars represent mean ± SE.

The amplification mechanism does not lead to a spontaneous retrieval of the memory in the absence of a cue. A memory pattern should be active only upon retrieval, and should remain inactive otherwise. In attractor networks, instability occurs when the coupling between the cells is too strong, and as a result the equilibrium at rest becomes positive and thus unstable. Since the amplification mechanism is induced across the whole cell, and since the increased excitation is balanced by increased inhibition, it is not expected to affect the stability of the memory at rest. Indeed, the amplification of the attractor did not cause the memory to become unstable during rest in any of the simulations.

Induction of the amplification mechanism on neurons that compose a memory pattern satisfies the requirements of memory amplification mechanism. Using both simulations and balanced network attractor models we show that equally multiplying the strength of all excitatory and inhibitory synapses in all the neurons that compose a neuronal ensemble satisfies the requirements from a memory amplification mechanism: it multiplies the number of spikes emitted by the neuronal ensemble only when the ensemble is retrieved; it retains the composition of the neurons that compose the ensemble; it maintains the silence of the ensemble in the absence of a triggering cue; it increases the statistical strength of the information encoded by the ensemble; and it has a larger effect on a learned ensemble.

Increasing the strength of an engram increases its statistical strength and thus enables it to dominate other engrams. This led us to test the predictions of the theoretical model: if the increased intensity of the freezing response is due to the induction of the amplification mechanism on the fear engram, then blocking the amplification mechanism should reduce the freezing response, without deleting the engram itself.

Blocking CaMKII results in reduced power of the fear engram if and only when the amplification mechanism is already active

The complete dependence of the maintenance of the whole-cell synaptic enhancement on persistent CaMKII activation presents an opportunity to generate the following prediction: blocking CaMKII phosphorylation in vivo should strongly reduce the freezing level only on the 5th day when the amplification mechanism is induced, and should not have an effect on the 1st and 3rd days when the amplification mechanism is not yet induced.

A cannula was implanted into the LA of extensively trained mice (Fig. 8A) 2 weeks before fear training, and CaMKII blocker (tatCN21) or its scrambled control, tatCtr (scrambled CN21), was applied into the LA 2 h before the retrieval (Supplementary Fig. 5).

Application of tatCN21 5 days after training significantly reduced the mean freezing response to 0.35 ± 0.13 as compared with application of scrambled peptide tatCtr (0.58 ± 0.1, two-tailed-ttest $t_{13} = 3.55$, $P = 0.0039$, $n = 7$; Fig. 8B). The two groups did not exhibit differences on the 1st day (tatCN21: 0.59 ± 0.17; tatCtr: 0.53 ± 0.09; $t_{13} = 0.76$, $P = 0.46$).

Next, we tested the effect of tatCN21 on the 3rd day after training, when the amplification mechanism is still not induced. At this time point, administration of tatCN21 did not reduce the freezing response (tatCN21: 0.55 ± 0.2; tatCtr: 0.47 ± 0.16; two-tailed-ttest: $t_6 = 0.48$, $P = 0.64$; Fig. 8C). The two groups did not exhibit differences on the 1st day (tatCN21: 0.52 ± 0.1; tatCtr: 0.50 ± 0.16; $t_9 = 0.59$, $P = 0.5$).

We also tested the effect of tatCN21 on the 1st day after training when the amplification mechanism is still not induced. The freezing response on the 1st day after training when tatCN21was applied (0.60 ± 0.26, Fig. 8D) was similar ($t_9 = 0.21$, $P = 0.84$) to the freezing response when tatCtr was applied (0.57 ± 0.14). The two groups did not exhibit differences in the retrieval in adjustment to conditioning (tatCN21: 0.54 ± 0.16; tatCtr: 0.51 ± 0.15; $t_9 = 0.26$, $P = 0.79$).

The lack of effect of tatCN21 on the 1st and the 3rd days when the amplification mechanism is not yet induced indicates that its effect on the 5th day is mediated through the deletion of the amplification mechanism. Moreover, these results further demonstrate that CaMKII-dependent activation of memory amplification mechanism 5 days after training is correlated with strong fear response that dominates the behavior during the fear retrieval.

Discussion

In this combined electrophysiological, behavioral, and computational work, we demonstrate that crucial fear learning leads to the induction of an amplification mechanism on each of the cells that compose the fear engram, thereby leading to the amplification of the engram. Moreover, we show that only crucial fear engrams are amplified, as the amplification mechanism is not induced on neurons that compose the mild fear engram or on neurons from control groups. Behaviorally, the amplified fear engram was correlated with a strong and persistent freezing response that was preserved for 6 weeks, while the non-amplified fear engram was correlated with a sharp reduction in freezing response just 5 days after fear training. Accordingly, blocking the amplification mechanism using a CaMKII blocker dramatically reduced the freezing response 5 days after fear conditioning.

Engram amplification is conceptually different from engram formation

The fear engram that is formed during an auditory fear conditioning was shown to be allocated in the LA[31–33] and to correlate with freezing response. Moreover, it was shown that increasing the strength of an engram enabled it to dominate the network and, accordingly, the behavioral response [17,18 20]. Taken together, these findings support the hypothesis that induction of the amplification mechanism on each of the neurons that compose the fear engram in the LA intensifies the strength of the engram and thus intensifies freezing response. Indeed, local application of a CaMKII blocker reduced the freezing response in the extensively conditioned group back to the level of the mildly trained group, in which the fear engram was not amplified.

Whole-cell multiplication is implemented through a CaMKII persistent activation-dependent whole-cell increase of the conductance of all synaptic channels

Twofold increase in the conductance of all synaptic channels leads directly to a uniform scaling of the strength of all synapses in the neuron by a factor of nearly two, which is the essence of the amplification mechanism (Supplementary Fig. 1). Our results show that: (1) the synaptic enhancement is CaMKII dependent and mediated by increase in the $GABA_A$ and AMPAR synaptic channel conductance. (2) Both the effect of training and the effect of CaMKII blocker on the synaptic strength could be computationally simulated assuming a process where the strength of virtually all synapses was nearly doubled.

Notably, a CaMKII-dependent twofold increase in the conductance of the AMPA channel is in line with reports from previous works[24,25,34], where CaMKII-dependent phosphorylation of serine 831 on the c-tail of the AMPA channel switches the conductance from a low conducting state to a high conducting state, resulting in a twofold increase of the channel conductance. Additionally, CaMKII is known to phosphorylate $GABA_A$ receptors[35]. However, both the subunit composition and the location of the $GABA_A$ receptors appear to be important in determining the functional outcome[35], making it difficult to pinpoint directly the effect of CaMKII on the $GABA_A$ channel conductance.

The induction of the amplification mechanism is triggered by the training, which leads to the induction of the amplification mechanism 5 days later

The induction of the amplification mechanism was also observed in neurons from wild-type mice, where the fear engram was not retrieved before the electrophysiological experiments, suggesting that it is the training itself that triggers a process in which 5 days later the engram amplification mechanism is induced. This is supported by the observation that *arc*+ cells in the control group did not exhibit the amplification mechanism. Epigenetic modification can develop during several days and thus can explain the 5-day incubation period. Indeed, it was demonstrated that 5 days after fear conditioning there was a re-localization of large chromatin segments from inactive to permissive environments and reorganization of the promoter–enhancer interaction landscape[36]. This work offers a plausible explanation for the incubation time of 5 days observed here.

Calcineurin-dependent decrease of the synaptic $GABA_A$ channels

Increasing the diffusion of $GABA_AR$ leads to a decrease of their density at synaptic sites and thereby to a decrease of the amplitude of GABAergic mIPSCs[28]. The increase in $GABA_AR$ diffusion rate is correlated with an increase in Ca^{2+} influx and requires the calcineurin-mediated dephosphorylation of the γ2 subunit at serine 327[28]. This is in line with our observation where a calcineurin blocker restored the amplitude of the inhibitory synaptic events back to control values through increasing the number of $GABA_A$ receptors.

The fear engram is modified through two independent learning-induced processes

On the 5th day, the inhibitory synaptic events are modulated by two different processes: (1) a CaMKII-dependent process that nearly doubles the conductance of the $GABA_A$ receptors. (2) A calcineurin-dependent process that decreases the number of $GABA_A$ receptors by increasing their diffusion rate. These two processes are induced by different phosphorylation sites and are differently implemented; therefore, their effect is additive.

The calcineurin-dependent decreased strength of the inhibitory synapses in each of the fear engram cells modifies the excitation inhibition balance in these cells. The balance of excitatory and inhibitory membrane currents is essential for maintaining stability of cortical networks[37,38]. Indeed, it was found in the sensory cortex that reduced inhibition increased the width of the tuning curve and thus decreased its input specificity[39]. Thus, decreasing the power of synaptic inhibition only can lead to instability of the fear engram and thus to a spontaneous retrieval of the engram and therefore to generalization. The induction of the CaMKII and the calcineurin-dependent processes on the cells that compose the fear engram, promotes the fear engram into a dominant engram, and reduces its activation specificity. The behavioral effect of injecting a calcineurin blocker to the amygdala should be examined in future work.

The difference in freezing between the mild and extensive paired groups is minor at 1st day and large at the 5th day after training. Several works show that the freezing in the 1st day after conditioning is a result of the associative learning between the tone and the shock[40–42], which explains the similar freezing in both groups. Thus, before the amplification is induced the freezing response is similar, in the next 4 days the freezing reduces due to active forgetting[43] and increases due to the amplification in the 5th day in the extensively paired group only.

To conclude, our data demonstrate that 5 days after a crucial fear training, a unique mechanism that amplifies the neurons' spiking

response is selectively induced on each of the neurons that compose the fear engram. We have shown theoretically and experimentally that this process amplifies the strength of the fear engram, which leads to a substantial increased freezing response.

Methods

Animals

C57bl6 mice (20–30 g) aged 8–10 weeks (Harlan Laboratories) were housed separately at 22 °C in a 12 h:12 h light:dark cycle, with access to food and water (ad libitum). The behavioral paradigms used for the experiments were approved by the University of Haifa Institutional Committee for Animal Experiments under the regulations in accordance with National Institutes of Health guidelines.

For the transgenic mouse line, we used a genetically engineered mouse line expressing destabilized Venus fluorescent protein (dVenus) under the control of a transgenic immediate early gene (IEG) *arc* promoter (*arc*:Venus mice). The transgenic (*arc*::dVenus) line carried the same genetic background as the wild-type breed C57BL6. The local breeding colony of the transgenic mouse line was maintained by our laboratory, with access to food and water (ad libitum) at 22 °C in a 12 h:12 h light:dark cycle. Experiments were performed at the age of 8–10 weeks. All the experiments were performed during the light phase, when the animals were active. The behavioral paradigms used for the experiments were approved by the university of Haifa Institutional Committee for Animal Experiments under the regulations in accordance with National Institutes of Health guidelines.

Polymerase chain reaction to identify the IEG arc knock-in of the arc gene in the transgenic mice

The transgenic male carrying the genetic knock-in of *arc*::dVenus was backcrossed with the wild-type female of c57bl6 genetic background. Littermate genotyping was performed in order to segregate the *arc*::dVenus-positive animals. The segregated *arc*::dVenus-positive males were taken for behavioral experiments.

Fear training paradigm

Fear conditioning experiments were performed using Coulbourn Instruments. For conditioning a rectangular chamber was fitted with an electrifiable grid. Videos to monitor the behavioral freezing response of the animals were recorded using a camera (Fujifilm, model no-DF6HA-1B) connected to a computer. The animals were further divided into naïve, paired training and unpaired training groups. Mice in the naïve group underwent no handling or exposure to the training context. The paired animals underwent conditioning where they received six pairs of tone shock (a 35 s tone, conditioned stimulus [CS], 35 dB larger than background level; 1500 Hz) co-terminated with a shock of 1 mA for 750 ms (unconditioned stimulus [US]). The unpaired group also received six tones (CS) and six shocks (US) on two consecutive days, in an unpaired manner where the order of tone and shock was randomized.

Both the paired and the unpaired groups underwent 30 min of habituation without the presentation of any tone or shock 24 h prior to the conditioning training day. Animal groups from the paired training paradigm (CS + US) were further divided into extensive training and mildly trained groups.

Fear retrieval

The fear retrieval was performed in a different chamber, which did not include the electrifiable grid. The mice received the tone three times, and the fear response was quantified as the percentage of freezing during the tone. The percentage of freezing during the tone was used as a quantification of the strength of the fear memory.

Training was defined as the fear conditioning followed by a retrieval 1 day after conditioning.

Extensively trained group

The extensively trained group underwent 2 days of training, 6 trials each day. Each trial contained a pair of tone shock. The fear conditioning was followed by retrieval 1 day after the conditioning.

Mildly trained group

The animals in the mildly trained group underwent only 1 day of training of six trials. Each trial contained a pair of tone shock. The fear conditioning was followed by retrieval 1 day after conditioning.

Post analysis of the behavioral recordings

The freezing percentage was always and measured only in the retrieval context. The percentage of freezing was measured from the start of the tone until its completion. For our experiments, freezing measurements were obtained from three consecutive trials in the retrieval context and an average was taken as the final freezing percentage for the animal. Freezing was defined as total immobility except breathing movements that lasted at least 2 seconds.

Electrophysiological recordings

The c57bl6 wild-type litter was kept in the home cage until they were killed for electrophysiological study. The transgenic *arc*::dVenus had a destabilized half-life period of 5 h; hence the maximum visualization of the fluorescence from the activated neurons could be achieved only after 5 h from the time of retrieval. Thus, to visualize the fluorescence on the activated neurons, the mice underwent fear retrieval 5 h before sacrificing the animal.

Slice preparation

The animals were perfused before the brain was isolated from the skull. Coronal slices (300 μm) were obtained from the LA and the brain slices were kept for recovery over 2 h in oxygenated ACSF (95% O_2 plus 5% CO_2). The ACSF contained the following (in mM): NaCl 124, KCl 3, $MgSO_4$ 2, NaH_2PO_4 1.25, $NaHCO_3$ 26, $CaCl_2$ 2, glucose 10. The slices after recovery were placed in a recording chamber under an infrared differential interference contrast microscope, the slices were constantly perfused with ACSF at 30 °C. Whole-cell patch clamp recordings were obtained from the LA. All electrophysiological recordings were performed using Axopatch 1D (Molecular Devices) and the data were acquired using pclamp9 (Molecular Devices).

Drug application. All drugs were applied in the perfused Ringer's solution at the following concentrations: KN93 (10 μM); calcineurin blocker cyclosporine (1μM). The CaMKII cell-penetrating peptide inhibitor tatCN21 and its scrambled inactive control peptide, tatCtr (scrambled CN21; GL Biochem, Shanghai LTD), were applied via Ringer's solution at a concentration of 5 μM.

Miniature IPSC recording. To record $GABA_A$-mediated miniature response from the LA, the recording electrode contained the following (in mM): 140 cesium chloride, 1 EGTA, 6 KCl, 4 NaCl, 2 $MgCl_2$ and 10 HEPES; at pH 7.25 and 280 mOsm. In these conditions, the reversal potential of chloride is 0 mV, and thus strong $GABA_A$-mediated currents can be obtained at a holding potential of −60 mV. The oxygenated ACSF perfusion solution contained TTX (1 μM), DNQX (20 μM) and APV (50 μM) to block glutamatergic synaptic transmission via AMPA receptors, thus allowing recording of pure IPSC. Recordings of miniature spontaneous events were obtained.

Miniature EPSC recording. To obtain miniature excitatory recordings (mEPSCs the neurons were voltage clamped at a membrane potential of −80 mV[44]. At this voltage most NMDA receptors and voltage-dependent channels are closed. The recording electrode was filled with a solution containing (in mM): 140 K-gluconate, 1 EGTA, 6 KCl, 4

NaCl, 2 $MgCl_2$, and 10 HEPES; at pH 7.25 and 280 mOsm. Miniature excitatory postsynaptic recordings were recorded in the presence of (1 μM TTX).

Stability of the recordings

The stability of the recordings was examined by measuring the difference in the holding current at the beginning and at the termination of the recordings, and is summarized in supporting table 1. In addition, the current required to create a −5 mV step is summarized in supporting Table 1 as well.

Spike frequency recordings

For neuronal adaptation measurements, prolonged (1 s) depolarizing current steps were applied to the neurons via the recording electrode at V_{rest},. For each neuron, we first determined the current required to elicit a single spike in response to the 1 s depolarizing pulse ($I_{Threshold}$). This value is of course particular for each neuron and reflects its basic membrane properties, such as input resistance, resting potential and spike threshold. We then applied a depolarizing current with double intensity ($I_{Threshold}$ X 2) to elicit repetitive spike firing. Since the stimulus intensity for each neuron is determined by the current required to elicit a single action potential, the number of spikes generated by this pulse is a good measurement of the neuron's intrinsic excitability, as previously used[44–46].

Stereotaxic surgery

Surgery. The mice were anesthetized by a combination drug of fentanyl (final 0.05 mg/kg), midazolam (final 5.0 mg/kg) and medetomidine (final 0.5 mg/kg). Additionally, they were given carpofen painkiller before surgery. 100 μl per 10 g body weight was injected intraperitonially. They were restrained in a stereotaxic apparatus (Thor labs) and implanted bilaterally with cannula. Coordinates with reference to Bregma were (AP) + 1.4 mm (ML) ± 3.4 mm (DV) −4.5 mm. On completion of the surgery the cannulas were fixed in position with dental cement. A stylus (company, measurements) was capped on the guide cannula to prevent dust entering the cannula. Once the surgery is over, they were injected with antibiotics and pain killer (Norocarp, Baytril). Animals were allowed 5–7 days to recover from the stress of surgery before starting with their training or before undergoing experimental manipulations.

Microinjection. While recovering from the surgery, the animal was well habituated with the person performing the experiment to avoid stress while handling prior to microinjection. On the day of injection, the stylus cap was removed and an injection cannula (company, measurements) containing the drug was inserted through the guide cannula. The injection cannula was carefully lowered into the LA. The injection cannula was connected via tubing, filled with double distilled water with a small bubble separating the water from the drug (tatCN21 peptide), to a 10 μl Hamilton syringe. Driven by a microinjection pump, the solution was injected at 0.5 μl/min per LA per injection. Once the drug was injected, the guide cannula was re-capped with a stylus. For our experiments, we had two different batches of animals for each group. Each group of animals were further separated as animals that received tatCN21 peptide and those that received the scambled control peptide. After injection of the drug, we waited for 2 hours before obtaining any behavioral data from them. The details of the animal groups that received tatCN21 peptide and the control tatCN21 (tatCtr) peptide are discussed in detail in the results section.

Drug. There have been a few studies that have reported the use of tatCN21 peptide inhibitor to block CaMKII-dependent phosphorylation and its scrambled inactive control peptide, tatCtr (scrambled CN21; GL Biochem, Shanghai LTD) at a concentration of 1.5 μg/μl.

Statistical analyses

One-way, two-way and three-way ANOVAs were used to evaluate significance of difference between four populations (e.g. extensively trained, unpaired, naïve and mildly trained groups), following a test for normality. When the ANOVA test indicated that significant differences existed, a post hoc Tukey's test was performed to determine differences between each pair of the four groups.

Values are presented as mean ± SD throughout the text.

The statistical differences (p values) between the amplitude distribution curves were calculated using the Kolmogorov–Smirnov test (Fig. 3, and Supplementary Figs. 3 and 4).

Nonstationary fluctuation analysis

The averaged single-channel current and the average number of active channels were estimated using a peak-scaled non-stationary fluctuation analysis (NSFA) of mEPSCs[34]. The NSFA was applied on the events that were electrotonically nearby (10–90% rise-times <1.5 ms; 61 ± 14% of events in trained; 64 ± 16% in pseudo-trained). Using Mini Analysis Software (Synaptosoft Inc.), events (80–300 per each cell) were scaled and aligned by their peak, and their decay phase was divided to 30 bins. The single-channel current (i) and the number of channels (N) were calculated (using Mini Analysis Software) by fitting the theoretical relationship for the peak scaled variance (σ^2) after subtraction of the background variance ($\sigma_b{}^2$):

$$\sigma^2(t) = i \cdot I(t) - I(t)^2/N + \sigma_b^2$$

Only cells in which the fitting of the equation yielded an $R > 0.85$ were incorporated into the analysis.

The single-channel conductance (γ) was calculated using the equation

$$\gamma = \frac{i}{\upsilon_h - \upsilon_{rev}}$$

where υ_h is the holding potential (−80 mV) and υ_{rev} is the reversal potential of the AMPA channel (0 mV).

Histology

Tissue collection and histology. The PFA-fixed brains of mice from paired ($N = 3$) and unpaired ($N = 3$) groups were obtained for quantification of *arc*-positive cells in the LA region. Serial coronal brain sections (50 μm) were obtained using a vibratome (Leica VT1000s, Leica Biosystems). The brain sections were mounted on slides and cover slipped with DAPI+ mutant (E19-18, GBI Labs).

Microscopy and imaging

The native fluorescence of *arc::dVenus* was used to quantify dvenus+ cells. For visualization of *arc*-positive cells, fluorescent images were acquired through a 20× objective lens of Zyla camera attached to a Nikon Ti2 fluorescent microscope. The images were acquired in a blue filter for DAPI staining, and FITC for *arc::dVenus* transcribing cells.

Quantification

To analyze the *arc* expression in the LA, brain areas were defined using the Allen mouse brain atlas as reference. The *arc*-positive cells within the anatomical borders of LA were counted manually from both hemispheres in each slice of 50 μm thickness. The cell counts are expressed as average number of *arc*-positive cells across 10–15 slices in each animal.

Theoretical models

The theoretical models are fully described in the supplementary information.

Ethical approval
All experimental procedures were performed and animals were handled and used in the experiments in accordance with the guidelines set by the NIH and approved by University of Haifa Animal Care and Use Committee with ethical license nos. #749, 922U and 762/21. We confirm that we acknowledge the ethical guidelines set by The journal Nature Communication and the paper complies with the journal's ethical checklist.

Data availability
Source data are provided with this paper.

Code availability
Code is provided with this paper.

References

1. Han, J. H. et al. Selective erasure of a fear memory. *Science* **323**, 1492–1496 (2009).
2. Reijmers, L. G., Perkins, B. L., Matsuo, N. & Mayford, M. Localization of a stable neural correlate of associative memory. *Science* **317**, 1230–1233 (2007).
3. Ryan, T. J., Roy, D. S., Pignatelli, M., Arons, A. & Tonegawa, S. Memory. Engram cells retain memory under retrograde amnesia. *Science* **348**, 1007–1013 (2015).
4. Pignatelli, M. et al. Engram cell excitability state determines the efficacy of memory retrieval. *Neuron* **101**, 274–284 (2019).
5. Carrillo-Reid, L. & Yuste, R. Playing the piano with the cortex: role of neuronal ensembles and pattern completion in perception and behavior. *Curr. Opin. Neurobiol.* **64**, 89–95 (2020).
6. Frankland, P. W., Josselyn, S. A. & Köhler, S. The neurobiological foundation of memory retrieval. *Nat. Neurosci.* **10**, 1576–1585 (2019).
7. Dorst, K. E. & Ramirez, S. Engrams: from behavior to brain-wide networks. *Adv. Neurobiol.* **38**, 13–28 (2024).
8. Josselyn, S. A., Köhler, S. & Frankland, P. W. Finding the engram. *Nat. Rev. Neurosci.* **9**, 521–534 (2015).
9. Meissner-Bernard, C., Dembitskaya, Y., Venance, L. & Fleischmann, A. Encoding of odor fear memories in the mouse olfactory cortex. *Curr. Biol.* **29**, 367–380 (2019).
10. Kim, J., Kwon, J. T., Kim, H. S., Josselyn, S. A. & Han, J. H. Memory recall and modifications by activating neurons with elevated CREB. *Nat. Neurosci.* **1**, 65–72 (2014).
11. Lee, S., Park, J. & Smirnakis, S. M. Internal gain modulations, but not changes in stimulus contrast, preserve the neural code. *J. Neurosci.* **39**, 1671–1687 (2019).
12. Stettler, D. D. & Axel, R. Representations of odor in the piriform cortex. *Neuron* **63**, 854–864 (2009).
13. Town, S. M., Wood, K. C. & Bizley, J. K. Sound identity is represented robustly in auditory cortex during perceptual constancy. *Nat. Commun.* **9**, 4786 (2018).
14. Barbour, D. L. Intensity-invariant coding in the auditory system. *Neurosci. Biobehav Rev.* **35**, 2064–2072 (2011).
15. Kiani, R. & Shadlen, M. N. Representation of confidence associated with a decision by neurons in the parietal cortex. *Science* **324**, 759–764 (2009).
16. Krekelberg, B., van Wezel, R. J. & TD, Albright Interactions between speed and contrast tuning in the middle temporal area: implications for the neural code for speed. *J. Neurosci.* **26**, 8988–8998 (2006).
17. Beck, J. M. et al. Probabilistic population codes for Bayesian decision making. *Neuron* **60**, 1142–1152 (2008).
18. Khalvati, K., Kiani, R. & Rao, R. P. N. Bayesian inference with incomplete knowledge explains perceptual confidence and its deviations from accuracy. *Nat. Commun.* **12**, 5704 (2021).
19. Reuveni I, Ghosh S & Barkai E. Real time multiplicative memory amplification mediated by whole-cell scaling of synaptic response in key neurons. *PLoS Comput. Biol.* **13**, e1005306 (2017).
20. Ferguson, K. A. & Cardin, J. A. Mechanisms underlying gain modulation in the cortex. *Nat. Rev. Neurosci.* **21**, 80–92 (2020).
21. Reuveni, I., Lin, L. & Barkai, E. Complex-learning induced modifications in synaptic inhibition: mechanisms and functional significance. *Neuroscience* **381**, 105–114 (2018).
22. Gouty-Colomer, L. A. et al. Arc expression identifies the lateral amygdala fear memory trace. *Mol. Psychiatry* **21**, 364–375 (2016).
23. Collingridge G.L. Bi-directional modulation of AMPA receptor unitary conductance by synaptic activity. *BMC Neurosci.* **44**, 1471-2202-5-44 (2004).
24. Derkach, V., Barria, A. & Soderling, T. R. Ca2+/calmodulin-kinase II enhances channel conductance of alpha-amino-3-hydroxy-5-methyl-4-isoxazolepropionate type glutamate receptors. *Proc. Natl Acad. Sci. USA* **96**, 3269–3274 (1999).
25. Derkach, V. A. Silence analysis of AMPA receptor mutated at the CaM-kinase II phosphorylation site. *Biophys. J.* **84**, 1701–1708 (2003).
26. Ghosh, S., Reuveni, I., Lamprecht, R. & Barkai, E. Persistent CaMKII activation mediates learning-induced long-lasting enhancement of synaptic inhibition. *J. Neurosci.* **35**, 128–139 (2015).
27. Ghosh, S., Reuveni, I., Barkai, E. & Lamprecht, R. Calcium/calmodulin-dependent kinase II activity is required for maintaining learning-induced enhancement of α-amino-3-hydroxy-5-methyl-4-isoxazolepropionic acid receptor-mediated synaptic excitation. *J. Neurochem.* **136**, 1168–1176 (2016).
28. Fricke, S. et al. Fast regulation of $GABA_AR$ diffusion dynamics by Nogo-A signaling. *Cell Rep.* **29**, 671–684.e6 (2019).
29. Cho, H. Y. et al. Turnover of fear engram cells by repeated experience. *Curr. Biol.* **31**, 5450–5461 (2021).
30. Roudi, Y. & Latham, P. E. A balanced memory network. *PLoS Comput. Biol.* **3**, 1679–1700 (2007).
31. Davis, P. & Reijmers, L. G. The dynamic nature of fear engrams in the basolateral amygdala. *Brain Res Bull.* **141**, 44–49 (2018).
32. Schafe, G. E., Doyère, V. & LeDoux, J. E. Tracking the fear engram: the lateral amygdala is an essential locus of fear memory storage. *J. Neurosci.* **25**, 10010–10014 (2005).
33. Lüthi, A. et al. Neuronal signalling of fear memory. *Nat. Rev. Neurosci.* **5**, 844–852 (2004).
34. Benke, T. A., Lüthi, A., Isaac, J. T. & Collingridge, G. L. Modulation of AMPA receptor unitary conductance by synaptic activity. *Nature* **393**, 793–797 (1998).
35. Houston, C. M., He, Q. & Smart, T. G. CaMKII phosphorylation of the GABA(A) receptor: receptor subtype- and synapse-specific modulation. *J. Physiol.* **587**, 2115–2125 (2009).
36. Marco, A. et al. Mapping the epigenomic and transcriptomic interplay during memory formation and recall in the hippocampal engram ensemble. *Nat. Neurosci.* **12**, 1606–1617 (2020).
37. Brunel, N. Dynamics of sparsely connected networks of excitatory and inhibitory spiking neurons. *J. Comput Neurosci.* **8**, 183–208 (2000).
38. Van Vreeswijk, C. & Sompolinsky, H. Chaotic balanced state in a model of cortical circuits. *Neural Comput* **10**, 1321–1371 (1998).
39. Thiele, A., Herrero, J. L., Distler, C. & Hoffmann, K. P. Contribution of cholinergic and GABAergic mechanisms to direction tuning, discriminability, response reliability, and neuronal rate correlations in macaque middle temporal area. *J. Neurosci.* **32**, 16602–16615 (2012).
40. Rogan, M. T., Stäubli, U. V. & LeDoux, J. E. Fear conditioning induces associative long-term potentiation in the amygdala. *Nature* **390**, 604–607 (1997).

41. Johansen, J. P. et al. Optical activation of lateral amygdala pyramidal cells instructs associative fear learning. *Proc. Natl Acad. Sci. USA* **107**, 12692–12697 (2010).
42. Suthard, R. L. et al. Engram reactivation mimics cellular signatures of fear. *Cell Rep.* **43**, 113850 (2024).
43. Hardt, O., Nader, K. & Nadel, L. Decay happens: the role of active forgetting in memory. *Trends Cogn. Sci.* **17**, 111–120 (2013).
44. Saar, D., Grossman, Y. & Barkai, E. Reduced after-hyperpolarization in rat piriform cortex pyramidal neurons is associated with increased learning capability during operant conditioning. *Eur. J. Neurosci.* **10**, 1518–1523 (1998).
45. Saar, D., Grossman, Y. & Barkai, E. Long-lasting cholinergic modulation underlies rule learning in rats. *J. Neurosci.* **21**, 1385–1392 (2001).
46. Awasthi, R., Chandra, N. & Barkai, E. Olfactory rule learning-induced enhancement in intrinsic neuronal excitability is maintained by shutdown of the cholinergic M-current. *Front. Cell Neurosci.* **16**, 934838 (2022).

Acknowledgements

This publication was made possible through the support of Grant 62056 from the John Templeton Foundation awarded to EB.

Author contributions

D.D.: data collection, formal analysis, investigation and writing—reviewing and editing. A.A.: data collection, formal analysis, investigation and writing—reviewing and editing. S.S.: histology and analysis. S.W.: investigation and writing—reviewing and editing. I.R.: data analysis, formal analysis, theoretical study, writing, reviewing and editing, supervision, conceptualization. E.B. equal contributor with I.R. data analysis, formal analysis, theoretical study, writing, reviewing and editing, supervision, conceptualization. All authors have read and approved the final version of the manuscript and agree to be accountable for all aspects of the work in ensuring that questions related to the accuracy or integrity of any part of the work are appropriately investigated and resolved. All persons designated as authors qualify for authorship.

Competing interests

The authors declare no competing interests.

Additional information

Supplementary information The online version contains supplementary material available at https://doi.org/10.1038/s41467-025-64854-5.

Correspondence and requests for materials should be addressed to Iris Reuveni.

Peer review information *Nature Communications* thanks the anonymous reviewer(s) for their contribution to the peer review of this work. A peer review file is available.